From the DEPARTMENT OF CLINICAL NEUROSCIENCE
Karolinska Institutet, Stockholm, Sweden

DEVELOPMENT OF PET RADIOLIGANDS SYNTHESIZED FROM IN-TARGET PRODUCED [^{11}C]METHANE

Jan Andersson

Karolinska Institutet

Stockholm 2010

Published by Karolinska Institutet.

Printed by University Service US-AB, Stockholm, Sweden

ISBN 978-91-7409-797-9

ABSTRACT

The aim of this thesis was two-fold. The first aim was to compare the specific radioactivity (SA) of positron emission tomography (PET) radioligands synthesized from in-target produced [^{11}C]methane ([^{11}C]CH_4) and [^{11}C]carbon dioxide ([^{11}C]CO_2). The second aim was to apply high SA [^{11}C]CH_4 in the development of PET radioligands for CNS targets such as the metabotropic glutamate receptor 5 (mGluR5), β-amyloid aggregates and the serotonin 1B (5-HT_{1B}) receptor system. PET is a molecular imaging technique that allows for high sensitivity imaging of particular targets or pathways in a living organism. One of the most commonly used radionuclides is carbon-11 ($t_{1/2}$ = 20.4 min) since it can be incorporated into many molecules without significant effect of biological activity and in addition the short half life allows for repeated injections in the same subject and day.

The $^{14}N(p, \alpha)^{11}C$ reaction on N_2–O_2 or N_2–H_2 gaseous systems during proton bombardment allows for the production of [^{11}C]carbon dioxide ([^{11}C]CO_2) and [^{11}C]methane ([^{11}C]CH_4). Compared to the more common in-target produced [^{11}C]CO_2, the [^{11}C]CH_4 resulted in a mean 6 fold to 17 fold increase of SA for four different PET radioligands synthesized from [^{11}C]methyl iodide ([^{11}C]CH_3I). For the dopamine D2 antagonist [^{11}C]raclopride, we obtained an average SA of 3908 GBq/μmol at the end of bombardment for the last 52 productions, which is a 32-fold increase compared to using the [^{11}C]CO_2 target. The mean SA of a radioligand synthesized from hydrogen [^{11}C]cyanide ([^{11}C]HCN) was 398 GBq/μmol when produced from the [^{11}C]CH_4 target, which is about nine times higher than from [^{11}C]CO_2. The reasons for the higher SA can to the greatest extent be attributed to [^{11}C]CO_2 being more sensitive to isotopic dilution from CO_2 in the air.

The hydroxyamidine [^{11}C]Ximelagatran, and the novel mGluR5 radioligand [^{11}C]AR-P135003 were prepared using palladium mediated ^{11}C-cyanation in high yield. There was high brain exposure of [^{11}C]AR-P135003 in cynomolgus monkey with a regional uptake that was in accordance with the known distribution of mGluR5.

The candidate amyloid PET radioligand [^{11}C]AZD2184 was successfully labeled by a two step radiosynthesis. Examination in monkey brain demonstrated sufficient brain exposure of [^{11}C]AZD2184 (2 – 3% of injected dose) with relatively low levels of white matter retention and may thus provide improved contrast compared to currently used PET radioligands for visualization of amyloid plaques.

Eight carboxamide radioligands from three different core structures aimed for visualization of the 5-HT_{1B} receptor were examined by PET in monkey and radiometabolites were measured in plasma. Lipophilicity was a physicochemical property showing relation to brain exposure and non-specific binding. [^{11}C]AZ10419369 was the most promising radioligand, showing high uptake of radioactivity in regions rich in 5-HT_{1B} receptors and low uptake in cerebellum resulting in relatively high binding potentials. The reported development program led to the identification of the first successful PET radioligand for visualization of 5-HT_{1B} receptors in the human brain.

In conclusion, we have shown that in-target produced [^{11}C]CH_4 makes it possible for the routine ^{11}C-labeling of PET radioligands with high SA. We utilized [^{11}C]CH_3I and [^{11}C]HCN synthesized from in-target produced [^{11}C]CH_4 in PET radioligand development programs where high SA radioligands for the mGluR5, β-amyloid and the 5-HT_{1B} were successfully developed.

Nothing in life is to be feared. It is only to be understood.

Marie Curie

To Candice

LIST OF PUBLICATIONS

I. Andersson J, Truong P, Halldin C. In-target produced [^{11}C]methane: Increased specific radioactivity. 2009, Applied Radiation and Isotopes 67:106-110.

II. Airaksinen AJ, Andersson J, Truong P, Karlsson O, Halldin C. Radiosynthesis of [^{11}C]Ximelagatran via palladium catalyzed [^{11}C]cyanation. 2008, Journal of labeled compounds and radiopharmaceuticals 51:1-5.

III. Andersson J, Seneca N, Truong P, Wensbo D, Raboisson P, Farde L, Halldin C. Palladium mediated [^{11}C]cyanation of the mGluR5 radioligand [^{11}C]AR-P135003: Characterization in the non-human primate brain. Manuscript.

IV. Andersson J, Varnäs K, Cselényi Z, Gulyás B, Wensbo D, Finnema SJ, Swahn B-M, Svensson S, Nyberg S, Farde L, Halldin C. Radiosynthesis of the candidate β-amyloid radioligand [^{11}C]AZD2184: PET examination and metabolite analysis in cynomolgus monkeys. 2010, Synapse, In Press.

V. Andersson J, Pierson ME, Finnema SJ, Gulyás B, Heys R, Elmore CS, Farde L, Halldin C. Development of radioligands for the 5-HT$_{1B}$ receptor: Radiosynthesis, characterization in the cynomolgus monkey brain and analysis of metabolism for eight potential PET radioligands. Manuscript.

VI. Pierson ME*, Andersson J*, Nyberg S, McCarthy DJ, Finnema SJ, Varnäs K, Takano A, Karlsson P, Gulyas B, Medd AM, Lee CM, Powell ME, Heys JR, Potts W, Seneca N, Mrzljak L, Farde L, Halldin C. [^{11}C]AZ10419369: A selective 5-HT$_{1B}$ receptor radioligand suitable for positron emission tomography (PET). Characterization in the primate brain. 2008, Neuroimage 41:1075-1085.

* Authors contributed equally to the manuscript.

CONTENTS

LIST OF ABBREVIATIONS

^{11}C	Radioactive, neutron deficient isotope of carbon
[^{11}C]CO_2	[^{11}C]carbon dioxide
[^{11}C]CH_4	[^{11}C]methane
[^{11}C]CH_3I	[^{11}C]methyl iodide
[^{11}C]CH_3OTf	[^{11}C]methyl triflate
[^{11}C]HCN	Hydrogen [^{11}C]cyanide
5-HT	Serotonin
α	Alpha particle
Aβ	Amyloid beta peptide
AD	Alzheimer's disease
Alpha particle	Positive helium ion (He^{2+})
BBB	Blood brain barrier
B_{max}	Binding maximum i.e. total receptor density
BP	Binding potential
Bq	Bequerel, SI derived unit of radioactivity
Carrier	Non radioactive form of radioligand/radiotracer
CT	Computed tomography
CNS	Central nervous system
Cyclotron	Particle accelerator
DMSO	Dimethyl sulfoxide
EOS	End of synthesis
EOB	End of bombardment (irradiation)
Ex vivo	"out of the living" e.g. tissue
FDA	Food and Drug Administration
Hot-cell	Lead shielded containment box
HPLC	High performance liquid chromatography
HR	High resolution
Hydrophilic	Polar, tendency to dissolve well in water
ICRP	International Commission on Radiological Protection
ID	Injected dose
In vitro	"in flask" i.e. in the test tube
In vivo	"in life" i.e. in the organism
IV	Intravenous
Kryptofix (K2.2.2)	4,7,13,16,21,24-hexaoxa-1,10-diazabicyclo [8.8.8]-hexacosane
Lipophilic	Non-polar, tendency to not dissolve well in water
LogP	Logarithm of partition coefficient octanol/water
MeCN	Acetonitrile
MeV	Mega electron volt
mGluR	Metabotropic glutamate receptor
MRI	Magnetic resonance imaging
OLINDA	Organ level internal dose assessment

OTf	Triflate, trifluoromethanesulfonyl
p	Proton
$Pd(PPh_3)_4$	Tetrakis(triphenylphosphine)palladium(0)
Pgp	P-glycoprotein (an efflux transporter)
PET	Positron emission tomography
RCY	Radiochemical yield
ROI	Region of interest
RT	Room temperature
SA	Specific radioactivity
Spatial	Relating to space
SPECT	Single photon emission computed tomography
SSRI	Selective serotonin release inhibitor
Stdev	Standard deviation
SUV	Standard uptake value
$t_{1/2}$	Half-life
TAC	Time activity curve
Temporal	Relating to time
TMP	2,2,6,6-Tetramethylpiperidine

1 INTRODUCTION

1.1 THE PET TECHNIQUE

Molecular imaging is a set of non-invasive techniques that enables the visualization of cellular function and molecular processes in the living organism. The imaging modalities of magnetic resonance imaging (MRI), optical imaging and nuclear imaging are emerging as key molecular imaging techniques because of their ability to detect molecular events when combined with contrast agents with sufficient sensitivity, specificity, temporal resolution and spatial resolution[1]. The nuclear imaging methods, positron emission tomography (PET) and single photon emission computed tomography (SPECT), require radiolabelled probes (radioligands or radiotracers) to be administered prior to the imaging measurement, which enables the specific visualization of certain proteins or biological processes in the living human being[2]. The other common tomography technique, X-ray computed tomography (CT), is not a molecular imaging technique as it can only give anatomical information and no functional information about molecular processes.

For *in vivo* investigations in humans, PET has the advantage of higher sensitivity and spatial resolution compared to SPECT[3] (3.8 mm for the PET camera used in this thesis and 8 mm for SPECT cameras) as well as better means of quantification due to more accurate scatter and attenuation correction. MRI has a lower sensitivity than PET, and is therefore not suitable for receptor studies since the higher mass will saturate available receptors[4].

The limitations of the PET technique are in large due to the short half-life of the positron emitting radionuclides used. The radionuclides have to be produced by a cyclotron adjacent to or at least in the regional area of the PET camera. The cyclotron and the equipment and laboratory space required for radiochemistry makes necessary for large investments. In contrast, the most commonly used SPECT radionuclide, ^{99m}Tc, is available from less expensive and commercially available generators.

The PET technique has application in our understanding of biological processes in a living system, with particular relevance in understanding disease pathology, progression and diagnosis, as well as in drug development. In PET, a molecule is tagged with a short-lived positron emitting radionuclide, and these labeled compounds are referred to as radioligands or radiotracers. One of the most commonly used radionuclides is carbon-11 ($t_{1/2}$ = 20.4 min) since it can be incorporated into many molecules including endogenous substances and pharmaceutical drugs without significant effect on biological activity, and in addition the short half life allows for repeated injections in the same subject and day. The radioligand or radiotracer is administered into the living organism that is under study and the ^{11}C -radionuclide decays by the transformation of a proton into a neutron to ^{11}B and with the emission of a positron and a neutrino. The positron will inevitably encounter an electron after traveling a few mm in the tissue which leads to annihilation of the two particles and two gamma photons (511 keV) are emitted in opposite directions of 180°. The photons are detected by a PET camera, and every event of coincidence is registered. Three dimensional images can be constructed by a computer to reveal the distribution of radioactivity over time. Another radionuclide that is commonly used in PET is ^{18}F ($t_{1/2}$ = 110 min).

Today the major clinical application for PET is in oncology and especially the tracer [^{18}F]fluorodeoxyglucose ([^{18}F]FDG) is widely used[5]. In addition to oncology,

clinical PET has also been proven useful in cardiology studying stroke[6] and neurology in the studies of e.g. Parkinson's[7] and Alzheimer's diseas[8]. In research it can be used to examine links between specific biological processes or proteins and different diseases.

PET is also useful in drug development, either by labeling the actual drug and e.g. assess whether a drug reaches the target organ or investigation of the interaction between the drug and enzymes or receptors. Such a study is known as a 'microdose' study since the PET technique enables the (radiolabeled) drug to be administered at very low doses[9-11]. This reduces the risk associated with toxicity of the drug, and can speed up the process of drug development from *in vitro* studies to *in vivo* studies in non human subjects to investigations in human subjects[12]. Another, indirect, way is to use a known radioligand and administer the drug (either as pre-treatment or displacement) and look at the perturbation the drug has on the system compared to baseline condition[13, 14].

1.2 DEVELOPMENT OF CNS PET RADIOLIGANDS

The success of a PET measurement depends to a large extent on the radioligand used in the experiment. It is necessary to use a PET radioligand that is specific for the certain protein or the biological process that you are interested in. Although the development of CNS PET radioligands began almost three decades ago there are today only a few established radioligands for a small number of targets. For the vast majority of CNS targets there exists no radioligand suitable for *in vivo* PET measurements. The development of PET radioligands is a multidisciplinary field and one can argue that physics, radiochemistry, medicinal chemistry, biology, pharmacology, drug metabolism, mathematics and regulatory affairs all are important disciplines necessary for the successful radioligand development program.

For a radioligand to be useful in human CNS PET studies the information collected by the PET camera needs to be suitable for quantitative analysis, otherwise the information is of little value for clinical investigations. The outcome measure of a PET experiment is usually the binding potential (BP), and for good quantification of the BP, the radioligand is required to possess some key properties[15-18]. These include high binding affinity for the target receptor, selectivity over other receptors and a high signal to noise ratio which depends upon both the affinity of the radioligand and the quantity of non-specific binding. The density of target proteins (B_{max}) is also an issue to consider, as this will influence the affinity (K_d) and selectivity needed by a successful radioligand. B_{max} should clearly exceed the K_d of the radioligand for good image contrast, a ratio of 5 between the two parameters can be used as an initial guideline[19]. Another important parameter is the lipophilicity of the compound; it impacts (but is not the sole affecting factor of) the plasma free fraction, brain exposure and the non specific binding. The specific binding equilibrium needs to be reached within a reasonable scan time, and if everything else is equal, higher affinity results in a longer required scan time. The specific radioactivity (SA) for the radioligand is required to be sufficiently high to produce negligible receptor occupancy (generally this means occupancy lower than 5%). The radiolabelled metabolites formed from the radioligand should not bind to the receptor of interest, and ideally not cross the BBB although if they do quantification is still possible. PET radioligands differ in properties compared to radioligands used in *in vitro* studies since they need to pass the BBB and bind reversibly to the target with kinetics allowing it to wash out from the brain within the scan time.

1.3 ^{11}C-PRODUCTION AND LABELING OF PET RADIOLIGANDS

Several nuclear reactions can be used to produce ^{11}C, amongst these the ^{14}N(p, α)^{11}C reaction is by far the most commonly used. A cyclotron (particle accelerator) is used for the irradiation of nitrogen gas. The ^{11}C-species that is formed reacts readily if a small amount of oxygen (< 2.0%) or hydrogen (5% - 10%) is available in the target gas and the primary precursors [^{11}C]carbon dioxide ([^{11}C]CO_2) or [^{11}C]methane ([^{11}C]CH_4) are formed, respectively. The in-target production of [^{11}C]CH_4 is generally achieved with higher SA while the radiochemical yield is lower compared to the production of [^{11}C]CO_2[20]. [^{11}C]CH_4 can also be formed using the classic nickel catalyzed hydrogenation of [^{11}C]CO_2[21] and in the opposite way, [^{11}C]CO_2 can be formed in an online preparation from [^{11}C]CH_4 using Cobalt (II,III) oxide[22].

[^{11}C]CH_4 has to be converted into more reactive forms (secondary precursors) to be useful in radiochemistry reactions. In this thesis [^{11}C]CH_3I and [^{11}C]HCN were employed as secondary ^{11}C-labeling precursors. Typically the production of [^{11}C]CH_3I is based on production of [^{11}C]CO_2 in a gas target, with subsequent reduction using lithium aluminum hydride and conversion to [^{11}C]CH_3I using hydriodic acid[23]. This method is often referred to as the 'wet' method. [^{11}C]CH_3I can also be obtained using gas phase iodination of [^{11}C]CH_4 in a radical reaction initiated at 720°C. The gas phase method can be utilized in a single pass method[24, 25] or by recirculating the unreacted [^{11}C]CH_4 to acquire higher conversion yields[26]. In short, the 'wet' method makes it possible to obtain high radiochemical yields while the specific radioactivity of the [^{11}C]CH_3I often is low (see below). The gas phase method can provide higher specific radioactivity of the labeling precursor whereas the drawback would be relatively low conversion yields.

[^{11}C]HCN is available from [^{11}C]CH_4 by reaction with ammonia (NH_3) over a platinum catalyst[27].

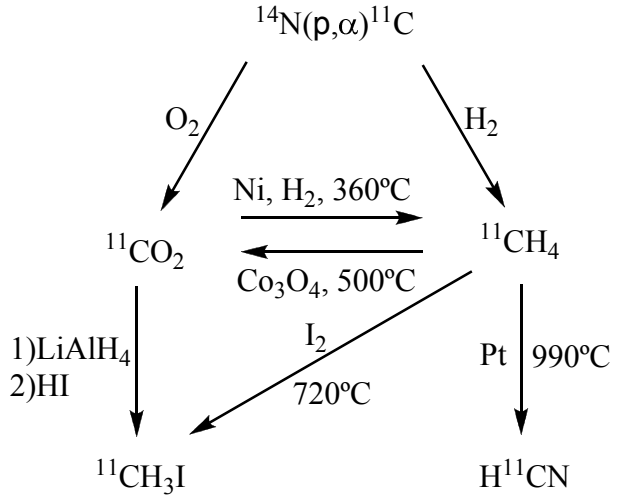

Scheme 1. Routes to produce the secondary ^{11}C-labeling precursors [^{11}C]CH_3I and [^{11}C]HCN.

The radiosynthesis to incorporate the ^{11}C-label into the PET radioligand has to be performed in automated systems within a hot-cell to minimize the radiation burden for personnel. Due to the short half life of ^{11}C, the incorporation has to be performed in a rapid manner. As a rule of thumb the radiosynthesis including purification and formulation should be performed within three half-lifes of the radionuclide, which would mean approximately 60 minutes for ^{11}C. Therefore it is of advantage if the

radiolabel can be introduced in the molecule as late as possible in the reaction sequence of the synthesis. Using large excess of precursor compared to the labeling agent and the use of high precursor concentration in small volumes can promote faster reaction times.

In this thesis [^{11}C]methyl iodide ([^{11}C]CH_3I) and hydrogen [^{11}C]cyanide ([^{11}C]HCN) were employed as secondary labeling precursors. [^{11}C]CH_3I is most widely used in methylation reactions, and the reactivity of the electrophilic carbon can be enhanced by preparing [^{11}C]methyl triflate ([^{11}C]CH_3OTf) in an on-line process[28, 29]. [^{11}C]CH_3I has also been used in wittig reactions[30], in transition metal mediated reactions such as the Suzuki[31] and Stille[32] couplings and it can be utilized to produce other labeling agents such as [^{11}C]methyl lithium[33], [^{11}C]nitroalkanes[34], [^{11}C]methanesulfonyl chloride[35], [^{11}C]methylmagnesium iodide[36] and triphenylarsonium [^{11}C]methylide[37]. [^{11}C]HCN can be used in aromatic substitution reactions to introduce a nitrile functionality. The nitrile can subsequently be transformed into a carboxylic acid, primary amine or amide and thus introduces a multi-functionality[38].

1.4 SPECIFIC RADIOACTIVITY

For commonly used PET radioligands with moderate binding affinity, the occupancy of the tracer itself is usually not a problem. However, high binding affinity (picomolar) radioligands such as the dopamine D2 receptor ligand [^{11}C]FLB 457 may introduce considerable occupancy even at very small injected masses[39]. The mass of radioligand that is administered in a PET measurement is dependent on how much radioactivity per unit mass of radiolabelled compound that is obtained. This is referred to as specific radioactivity (SA) and is usually given in the unit of GBq/µmol.

The theoretical value of specific radioactivity can be calculated using the following equation:

$$SA = \frac{ln2}{t_{1/2}} N \qquad \textbf{Equation 1.}$$

where N is the number of atoms of the radioactive element. Using Avogadro's number we can calculate the theoretical SA in Bq/mol. From this equation it is also obvious that the theoretical SA only depends on the $t_{1/2}$ of the radionuclide (and not time) and that a shorter $t_{1/2}$ gives a higher theoretical SA. The theoretical value of SA for ^{11}C is 3.4×10^5 GBq/µmol. This SA is considerably higher than what is usually reported for PET radioligands in the literature (100 – 500 GBq/µmol), which means that the amount of unlabelled compound far exceeds the labeled compound in which case the SA will be a function of time and exponentially decline with the half-life of the radionuclide:

$$SA(t) = \frac{A(t)e^{-(ln2/t_{1/2})t}}{m} \qquad \textbf{Equation 2.}$$

where A(t) is the radioactivity at the time of measurement, t = time after radioactivity measurement, m = mass of compound. At very high SA, i.e. a ratio of unlabelled atoms to that of labeled atoms of ten or smaller is reached, the mass of the labeled species also has to be taken into account for in the SA calculations[40].

The production of [^{11}C]CO_2 often results in good radiochemical yields and high radioactivity, however there remains to be a problem with the specific radioactivity (SA) of the produced labeling precursor. The Earth's atmosphere contains about 0.038% CO_2, and despite strong efforts to prevent it, this often contaminates the labeled precursor resulting in low SA. The isotopic dilution can occur both during the

radionuclide production from the target gas and holder as well as from the reagents, valves and tubings used in the radiosynthesis. *In situ* production of [^{11}C]CH_4 in the target should provide higher specific radioactivity as long as the hydrocarbon content of the target gases is less than the corresponding CO_2 that may enter the system from different sources[41]. In addition this method eliminates potential sources of decreased SA by avoiding the use of $LiAlH_4$/THF[42] which is used in the 'wet' method to produce [^{11}C]CH_3I from [^{11}C]CO_2.

1.5 THE METABOTROPIC GLUTAMATE RECEPTOR 5 (MGLUR5)

The mGluR5 is believed to be an important therapeutic target for a number of CNS disorders[43] including anxiety (maybe in interaction with the serotonergic system)[44], schizophrenia[45], Parkinson's disease[46], Alzheimer's disease[47], addiction[48], epilepsy[49] as well as various pain states.

Glutamate is the main excitatory neurotransmitter in the brain, acting through ionotropic (NMDA, kainate and AMPA) and metabotropic (mGlu) receptor subtypes. The mGluR5 is one out of eight subtypes of the mGlu receptors that have been cloned to date and it is coupled to phospholipase C and regulate neuronal excitability[50]. The structure of the mGluR5 is divided into several distinct regions: Venus flytrap mechanism, cystein rich domain, heptahelical domain and an intracellular C-terminal region[43, 50]. The Venus flytrap mechanism consists of a large extracellular region made up of two globular domains with a hinge region that is responsible for agonist binding and activation of the G-protein through conformational change of the receptor upon agonist binding. While glutamate binds to the large extracellular region, the action of non-competitive antagonists, aka negative allosteric modulators, such as 2-methyl-6-phenylethynyl-pyridine (MPEP)[51] and 2-methyl-4-(pyridin-3-ylethynyl)thiazole (MTEP) [52], is within the TM regions, specifically TMIII and TMVII[53]. It is speculated that negative allosteric modulators binding within the TM region of mGluR5s stabilize the inactive state of the receptor and therefore inhibit the constitutive activity.

Immunohistochemical staining has shown that the distribution of the mGluR5 is widely expressed with the highest density in the olfactory bulb, caudate/putamen, lateral septum, cortex and hippocampus[54]. In cerebellum, only a small amount of mGluR5 mRNA is detected.

The therapeutic potential of a drug targeting mGluR5 has led to recent advances in the development of negative allosteric modulators. Most ligands that are being developed are diaryl alkynes, based on the structure of the prototypical mGluR5 antagonists MPEP[51] and MTEP[52]. There has been a lack of selective PET radioligands for the mGluR5, however in recent years successful PET imaging of mGluR5 has been reported for 3-(6-Methyl-pyridin-2-ylethynyl)-cyclohex-2-enone-*O*-[^{11}C]-methyloxime ([^{11}C]-ABP688)[55] and [^{18}F]3-Fluoro-5-[(pyridin-3-yl)ethynyl]benzonitrile ([^{18}F]F-PEB)[56]. The compound reported in this thesis, 3-fluoro-5-(3-(5-fluoropyridin-2-yl)-1,2,4-oxadiazol-5-yl)benzo-[^{11}C]-nitrile ([^{11}C]AR-P135003), belongs to a novel class of mGluR5 ligands which does not depend on the presence of an alkyne moiety (Figure 1).

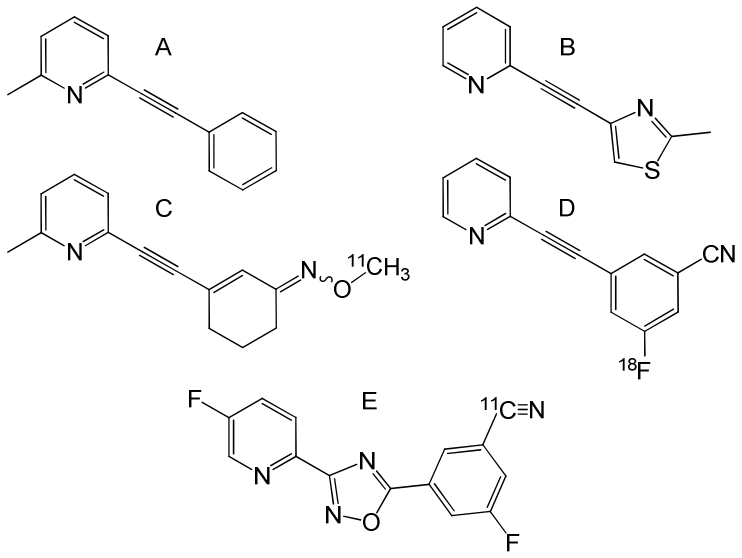

Figure 1. Structures of A) MPEP, B) MTEP, C) [^{11}C]ABP688, D) [^{18}F]F-PEB and E) [^{11}C]AR- P135005.

AR-P135003 has in binding studies showed high affinity (K_D = 3.8 ± 0.7 nM) for the human mGluR5 and evidence support the contention that AR-P135003 bind to the same allosteric binding site of the mGluR5 as MPEP. In addition, selectivity screenings has shown that AR-P135003 is highly selective for the mGluR5 over other mGlu receptors as well as a broad panel of other targets (Table 1).

Table 1. Molecular weight, lipophilicity, affinity and selectivity data for the potential mGluR5 radioligand [^{11}C]AR-P135003.

Compound	MW	cLogD	Affinity	Selectivity	
	(g/mol)	(pH = 7.4)	(mGluR5, K_D, nM)	other mGluR's	136 other targets
AR-P135003	283.22	2.74	3.8 ±0.7	>1000	>100

1.6 IMAGING OF AMYLOID PLAQUES

Alzheimer's disease (AD) is the most common cause of dementia and one of the most widespread illnesses of later life. Early cognitive and behavioral symptoms of AD are difficult to distinguish from normal signs of aging, and most patients are therefore not accurately diagnosed until neuronal damage becomes extensive. Although currently used drugs may provide temporary relief from symptoms, no treatments are available to halt disease progression[57]. The best hope for improvement might be to detect the disease at an early stage, and initiate treatment before the brain damage is widespread. Senile plaque accumulation is associated with the pathogenesis of AD[58]. The plaques consist of β-amyloid (Aβ) aggregates and imaging of these aggregates in the living human brain is currently a main focus in research on AD. Detecting deposits of β-amyloid using PET at an early stage could lead to earlier and more conclusive diagnosis of AD. In addition, imaging tools may serve to confirm proof of mechanism for new disease-modifying drug therapies.

Among the PET radioligands that have been investigated to date the most extensively studied radioligand is [^{11}C]PIB (2-(4-(methyl-^{11}C-amino)phenyl)benzo[d]thiazol-6-ol, [^{11}C]6-OH-BTA-1), a derivative of the amyloid binding dye Thioflavin-T (2-(4-(dimethylamino)phenyl)-3,6-dimethyl-benzo[d]thiazol-3-ium, Figure 2)[59-61]. Although PET imaging with [^{11}C]PIB has provided valuable new

information, the high degree of white matter retention displayed by [^{11}C]PIB may limit its use as a tool for early diagnosis of AD when plaque levels are relatively low.

A new potential radioligand for imaging of Aβ deposits, AZD2184 ((N-methyl)-2-(6-methylamino-pyridin-3-yl)-benzo[d]thiazol-6-ol, Figure 2), has recently been reported[62].

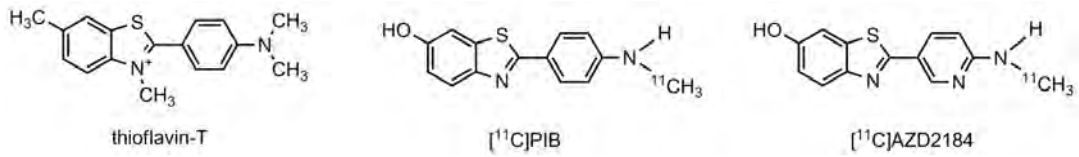

Figure 2. Structures of thioflavin-T and its labelled derivatives [^{11}C]PIB and [^{11}C]AZD2184.

AZD2184 displays high affinity for human amyloid fibrils in vitro (Kd = 8.4 ± 1.0 nM) and favourable brain uptake in rodents in vivo (1% of injected dose (ID) 2 min post injection)[62]. *In vitro* autoradiography has shown that while [^{3}H]AZD2184 and [^{3}H]PIB are mutually displaceable, [^{3}H]AZD2184 displays a higher signal to noise ratio by the feature of lower background binding. This in vitro profile might suggest an improved signal in PET compared to currently used radiotracers.

1.7 THE SEROTONIN 1B (5-HT$_{1B}$) RECEPTOR

Serotonin (5-hydroxytryptamine, 5-HT) is a neurotransmitter that mediates a wide range of effects by binding to multiple receptors in the human brain[63]. The serotonin 1B (5-HT$_{1B}$) receptor, plays a crucial role as an autoreceptor modulating synaptic release of serotonin[64]. In addition, 5-HT$_{1B}$ receptors serve as heteroreceptors modulating transmitter release in several non-serotonergic systems[65, 66].

Compounds that alter the reuptake or degradation of serotonin have long been used in the pharmacological treatment of many neuropsychiatric disorders[67]. Pharmacological and genetic studies give support for involvement of the 5-HT$_{1B}$ receptor subtype in the pathophysiology of anxiety, depression, aggressive behavior and substance abuse[68, 69] as well as in Alzheimer's disease[70]. Drugs specifically targeting the 5-HT$_{1B}$ receptor could thus have a role in the treatment of psychiatric disorders. For example, antagonists at the 5-HT$_{1B}$ autoreceptor may enhance serotonergic neurotransmission *in vivo*[71] and have shown antidepressant-like effects in animal models of depression[72].

The regional distribution of 5-HT$_{1B}$ receptors in the postmortem human brain has previously been examined using autoradiographic methods[73, 74]. These investigations found evidence for high densities of 5-HT$_{1B}$ receptors in the pallidum, substantia nigra, ventral striatum and visual cortex. It has been difficult to differentiate the 5-HT$_{1B}$ and 5-HT$_{1D}$ receptor subtypes in native systems since they are pharmacologically similar[75], however the 5-HT$_{1B}$ receptor is more highly expressed in brain tissue than the 5-HT$_{1D}$ receptor[76].

Drugs and ligands selective to the 5-HT$_{1B/1D}$ receptor proteins include the agonist zolmitriptan ((S)-5-((3-(2-(dimethylamino)ethyl)-1H-indol-5-yl)methyl)pyrrolidin-2-one)[77], a drug for the treatment of migraine headaches, the partial agonist GR127935 (*N*-(4-methoxy-3-(4-methylpiperazin-1-yl)phenyl)-2'-methyl-4'-(5-methyl-1,2,4-oxadiazol-3-yl)biphenyl-4-carboxamide)[78], the 5-HT$_{1B}$ selective inverse agonist SB-224289 ((2'-methyl-4'-(5-methyl-1,2,4-oxadiazol-3-yl)biphenyl-4-yl)(1'-methyl-6,7-dihydrospiro[furo[2,3-f]indole-3,4'-piperidine]-5(2H)-yl)methanone)[79] and the reference radioligand for *in vitro* autoradiographic studies, [^{3}H]GR125743 (*N*-(4-

methoxy-3-(4-methylpiperazin-1-yl)phenyl)-3-methyl-4-(pyridin-4-yl)benzamide)[80]. Previously, AR-A000002 ((R)-5-methyl-8-(4-methylpiperazin-1-yl)-*N*-(4-morpholinobenzyl)-1,2,3,4-tetrahydronaphthalen-2-amine) (Figure 3) has been shown to be a selective 5-HT_{1B} antagonist[81].

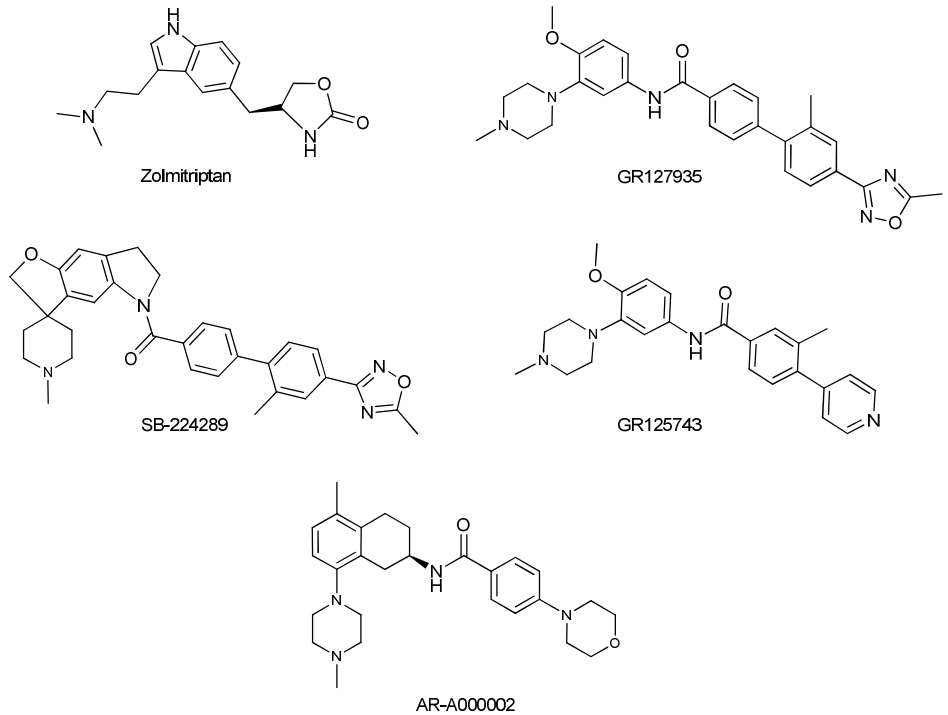

Figure 3. Structures of five reference compounds for $5HT_{1B}$-binding. The anti-migraine agonist Zolmitriptan, the partial agonist GR127935, the inverse agonist SB-224289, the reference ligand for *in vitro* studies GR125743 and the antagonist AR-A000002.

However, before the start of this thesis no suitable radioligands had been reported for *in vivo* imaging of 5-HT_{1B} receptors with PET. The development of a suitable 5-HT_{1B} receptor PET radioligand would facilitate the selection of drug candidates targeting this receptor, and enable the determination of dose-occupancy relationships for 5-HT_{1B} receptor-selective compounds. In addition, availability of a PET 5-HT_{1B} receptor radioligand could allow for clinical research on the pathophysiology of major psychiatric disorders.

2 AIMS

The aims of the present thesis were to compare the specific radioactivity (SA) of PET radioligands synthesized from in-target produced [^{11}C]CH_4 and [^{11}C]CO_2, and to utilize the obtained high SA [^{11}C]CH_3I and [^{11}C]HCN in the development of PET radioligands.

The two primary aims of the project were as follows:

1. To study the effect on specific radioactivity when using in-target produced [^{11}C]CH_4 compared to the more commonly used [^{11}C]CO_2.

   Paper I. A longitudinal comparison between in-target produced [^{11}C]CH_4 and [^{11}C]CO_2 and the effect on the SA of [^{11}C]CH_3I.

   Paper II. The set up of a reliable semi-automated system for the ^{11}C-cyanation of [^{11}C]Ximelagatran, including the use of in-target produced [^{11}C]CH_4 to assure high SA of the labeled radioligand.

   Paper III. Palladium mediated ^{11}C-cyanation of [^{11}C]AR-P135003 and its *in vivo* characterization. The radioligand was produced both from in-target produced [^{11}C]CH_4 (not included in the manuscript) and [^{11}C]CO_2.

2. To use the high SA [^{11}C]CH_4 in development of PET radioligands for the mGluR5, β-amyloid and 5-HT_{1B}.

   Paper III. The palladium mediated ^{11}C-cyanation of the mGluR5 antagonist [^{11}C]AR-P135003 and its *in vivo* characterization.

   Paper IV. The improved second generation amyloid radioligand, [^{11}C]AZD2184, was radiolabelled in two steps from high SA [^{11}C]CH_3I, and evaluated in cynomolgus monkey.

   Paper V. Radioligand development program for the 5-HT_{1B} receptor. *In vivo* PET measurements of eight PET radioligands.

   Paper VI. A more extensive characterization of the 5-HT_{1B} PET radioligand, [^{11}C]AZ10419369, and the first visualization of 5-HT_{1B} in the human brain.

3 MATERIALS AND METHODS

A brief summary of the general methods used during this thesis work are described here. For complete details the reader is referred to the copies of the full papers and manuscripts that follow.

3.1 RADIOCHEMISTRY

All irradiations were performed on a GEMS PETtrace cyclotron (GE, Uppsala, Sweden) using 16.4 MeV protons.

The [^{11}C]CO_2 target was a 78 mL aluminium target. The target gas used was 0.5% oxygen in nitrogen of scientific grade purity (99.9999%). Process gases used were nitrogen, hydrogen and helium of scientific grade (99.9999%). The gases were purchased from AGA GAS AB (Sundbyberg, Sweden).

The [^{11}C]CH_4 target used was a 78 mL aluminium target, with Havar foils (25μm) and graphite collimators. Cooling of the target body was achieved by a water system and the foil was cooled using He gas. 10% Hydrogen in nitrogen of scientific grade purity (99.9999%) was used as target gas. The gas was flushed through a nitrogen purifier (All Pure™ Alltech with specifications of <1ppb for CO, CO_2, O_2, H_2O and sulfur compounds and <3ppb for non methane hydrocarbons for a nominal inlet concentration of 50ppm) before reaching the target.

3.1.1 Production of [^{11}C]CH_3I

Starting from in-target produced [^{11}C]CO_2, [^{11}C]CH_3I was synthesized utilizing a GEMS MeI Microlab® system using previously reported procedures[82]. Briefly [^{11}C]CO_2 was reduced over shimalite nickel (Alltech) at 360°C with hydrogen to [^{11}C]CH_4 followed by gas phase halogenation to obtain [^{11}C]CH_3I.

Starting from in-target produced [^{11}C]CH_4, [^{11}C]CH_3I was produced according to previously published methods[26]. In short, [^{11}C]CH_4 was released and passed through a phosphorous pentoxide trap (to remove trace amounts of ammonia and water produced in the target) and collected in a Porapak Q trap cooled with liquid nitrogen. The nitrogen and hydrogen was flushed to waste using helium. Following collection, the [^{11}C]CH_4 was released from the trap by heating with pressurized air, into a recirculation system consisting of a micro diaphragm gas pump (NMP830KVDC, KNF Neuberger, Freiburg, Germany), three ovens, a Porapak Q trap and a Quartz tube containing iodine and ascarite. First the [^{11}C]CH_4 was pumped to the quartz tube where it was mixed with vapours from iodine crystals at 60°C and then reaction occured at 720ºC (Carbolite oven type: MTF 10/15G, GE Medical Systems, Sweden). After the reaction the iodine and HI were trapped in ascarite while the [^{11}C]CH_3I was collected in a porapak Q trap at room temperature and the unreacted [^{11}C]CH_4 was recirculated for three minutes (Figure 4). [^{11}C]CH_3I was released from the porapak Q trap by heating the trap using a home-built oven to 180°C.

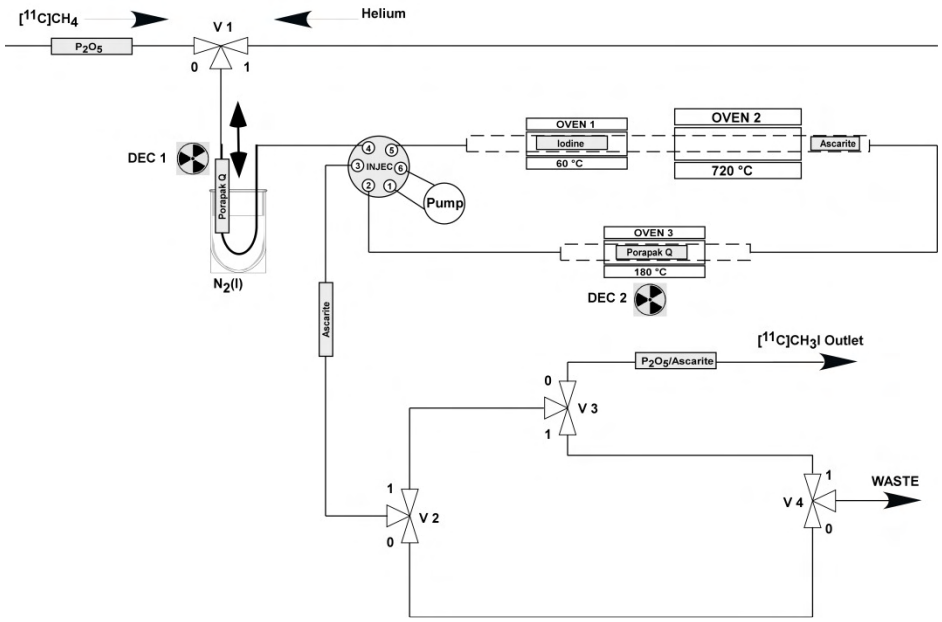

Figure 4. Circulation system for gas phase iodination.

3.1.2 Production of [^{11}C]HCN

[^{11}C]HCN was produced according to previously published methods[41]. In short NH_3 gas (flow 20-30 mL/min) was added to the produced (either from in-target production or the [^{11}C]CH_4 from hydrogenation of [^{11}C]CO_2) [^{11}C]CH_4 (200 mL/min) and the mixture was passed through a furnace (Carbolite, Hope Valley, UK) containing a quartz tube with a heated platinum wire (990˚C). The produced [^{11}C]NH_4CN was bubbled through H_2SO_4 (50%, 2 mL) at 65˚C to generate [^{11}C]HCN. A flowchart of the full synthesis module for ^{11}C-cyanations is shown in Figure 5.

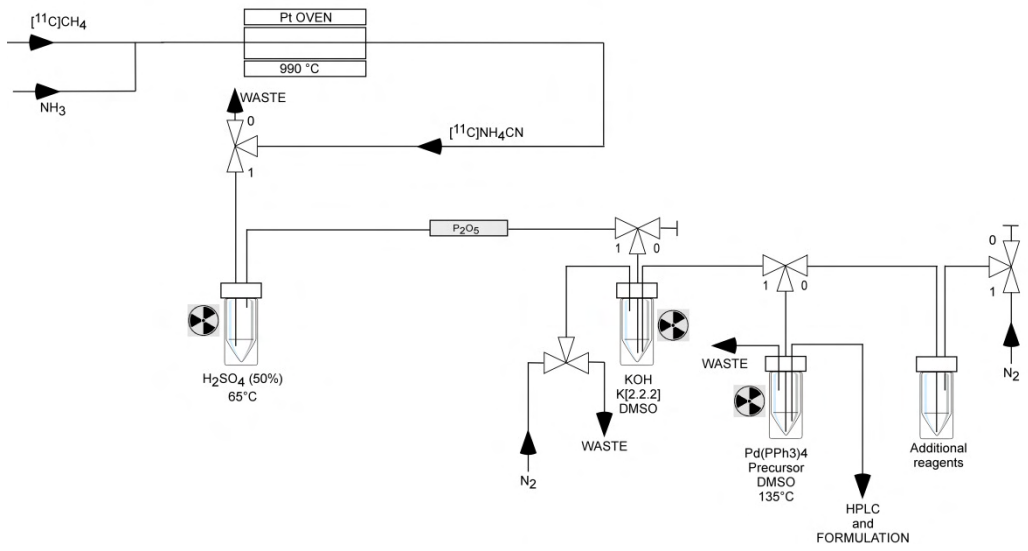

Figure 5. Schematic diagram of the radiochemistry apparatus for H^{11}CN production and subsequent labelling.

3.2 PET MEASUREMENTS

Cynomolgus monkeys (*Macaca fascicularis*), are housed in the Astrid Fagraeus Laboratory of the Swedish Institute for Infectious Disease Control (SMI), Solna, Sweden. The study was approved by the Animal Ethics Committee of the Swedish Animal Welfare Agency and was performed according to "Guidelines for planning, conducting and documenting experimental research" (Dnr 4820/06-600) of the Karolinska Institutet as well as the "Guide for the Care and Use of Laboratory Animals"[83].

Anesthesia was induced and maintained by repeated intramuscular (i.m.) injections of a mixture of ketamine hydrochloride (3.75 mg/kg/h, Ketalar®, Pfizer) and xylazine hydrochloride (1.5 mg/kg/h Rompun® Vet., Bayer) for the duration of each measurement. A head fixation system was used to secure a fixed position of the monkey´s head during the PET measurements[84]. Body temperature was maintained by Bair Hugger – Model 505 (Arizant Healthcare Inc., MN) and monitored by a rectal thermometer (Precision Thermometer, Harvard Apparatus, MA). Cardiac and respiratory rates were measured every 20 min. The monkeys were observed continuously during the PET experimental days. In each PET-measurement a sterile physiological phosphate buffer (pH = 7.4) solution containing radioligand was injected as a bolus into a sural vein during 5 seconds with simultaneous start of PET-data acquisition.

Radioactivity in brain was measured continuously for 93 minutes with the ECAT EXACT HR system (Siemens AG, Erlangen, Germany) according to a pre-programmed series of frames starting immediately after an intravenous injection of the radioligand. All acquisitions were acquired in 3D-mode[85]. A three-ring detector block architecture gave a 15 cm wide field of view. The transversal resolution in the reconstructed image was about 3.8 mm full width half maximum (FWHM) and the axial resolution was 3.125 mm. The attenuation correction of the data was obtained with the three rotating ^{68}Ge rod sources. Raw PET data were then reconstructed using the standard filtered back projection consisting of the following reconstruction parameters: 2 mm Hanning Filter, scatter correction, a zoom factor of 2.17 and a 128 x 128 matrix size[85]. The regions of interest were drawn on PET summation images representing radioactivity measured from 9 to 93 minutes after intravenous injection of radioligand.

All quantitative analysis calculations were based on the assumption that radioactivity in brain represents unchanged radioligand[86]. The fraction of radioligand in brain relative to the total amount of radioligand injected was calculated and plotted versus time after injection. The radioactivity concentration in the region of interest (ROI) for the whole brain was multiplied with the whole brain ROI volume (~65 mL), divided by the radioactivity injected and multiplied by 100 to obtain the percentage. Regional radioactivity concentrations were decay-corrected and normalized to injected radioactivity and body weight by use of % of standard uptake value (%SUV), where

$$\%\mathrm{SUV} = \frac{\%\ \text{injected activity}}{\text{brain tissue (ccm)}}\,\text{body weight (g)} \qquad \textbf{Equation 3.}$$

3.3 PLASMA METABOLITE STUDIES

The method for determination of the percentages of radioactivity corresponding to unchanged radioligand and labeled metabolites during the time of a PET

measurement was a modification of an HPLC method that has been used for other PET radioligands[87]. Blood samples (2 mL) were obtained venously from the monkey usually at 5, 15 and 30 minutes after injection of the radioligand. After centrifugation at 2000 g for 2 min, plasma was obtained (0.5mL) and mixed with acetonitrile (0.7mL). The mixture was centrifuged at 2000 g for 2 min and the supernatant (1 mL) was injected to a HPLC. The radioactivity in blood (2mL) and plasma (0.5 mL) were measured in a NaI well counter.

The radioactive peak having a retention time corresponding to the unchanged radioligand was integrated and its area was expressed as a percentage of the sum of the areas of all detected radioactive peaks.

4 RESULTS AND DISCUSSION

4.1 SPECIFIC RADIOACTIVITY: [^{11}C]CH_3I (PAPER I)

The in-target production of [^{11}C]CH_4 resulting in high SA radioligands prepared from [^{11}C]CH_3I has previously been described in the literature[25], but the aim of this study was to look at longitudinal data from the use of this method. The influence on the SA on four radioligands produced from in-target produced [^{11}C]CH_4 was related to the productions from in-target produced [^{11}C]CO_2. As model compounds [^{11}C]raclopride[88, 89], [^{11}C]MADAM[90], [^{11}C]PE2I[91] and [^{11}C]FLB 457[92, 93] were selected, mostly based on the frequent production of these radioligands in our lab. These radioligands were all labeled by heteroatom ^{11}C-methylations using methods that are well described in the literature[94]. The radioligands were prepared from both in-target produced [^{11}C]CO_2 and [^{11}C]CH_4 and the SA was measured on the final formulations and calculated to the end of bombardment (EOB).

The results obtained by switching to in-target produced [^{11}C]CH_4 was a 6- to 17-fold increase of SA for [^{11}C]raclopride, [^{11}C]MADAM, [^{11}C]PE2I and [^{11}C]FLB 457 (Table 2).

Table 2. Specific radioactivity (SA) for four radiopharmaceuticals.

	[^{11}C]Raclopride	[^{11}C]MADAM	[^{11}C]PE2I	[^{11}C]FLB 457
SA [^{11}C]CO_2	124	162	183	176
n	85	21	23	95
Min	9	28	24	5
Max	371	427	507	686
Synth time (min)	36	34	33	31
SA [^{11}C]CH_4	2335	2332	1097	1313
n	211	51	8	16
Min	180	345	442	126
Max	10231	16817	2387	6848
Synth time (min)	32	30	30	32

SA [^{11}C]CO_2 is the mean value of specific radioactivity of the radiopharmaceutical produced from [^{11}C]CO_2 given in GBq/µmol at the end of bombardment (EOB); SA [^{11}C]CH_4 is the SA of the radiopharmaceutical starting from target produced [^{11}C]CH_4; n is the number of productions; Min and Max are the lowest and highest measured SA respectively and the Synth time is the typical synthesis time for the productions.

The results for the [^{11}C]CH_4 target reported in Table 2 shows the mean SA over 3.5 years of productions of the four radioligands. The reasons for the higher SA can to the greatest extent be attributed to [^{11}C]CO_2 being more sensitive to isotopic dilution from CO_2 in the air, than what the influence of environmental contamination of CH_4 is likely to have on the SA. However, it is still very important to keep the target chamber free from air since contamination by cold carbon species could result in lower SA. The target was thus kept under pressure at all times. The nickel catalyzed step to produce [^{11}C]CH_4 from [^{11}C]CO_2 was obviously not necessary when [^{11}C]CH_4 was produced *in situ*, which also excluded one step for possible contaminations which could have resulted in lower SA. The target gas and the helium carrier gas can also introduce carbon-containing contaminants; consequently high purity of all gases was important.

The N_2-H_2 target gas was flushed through a nitrogen purifier before reaching the target. No such gas purifier was used for the [^{11}C]CO_2 target. Interestingly, no significant improvement of the SA was found when productions were performed after pre-irradiations and therefore no pre-irradiations were carried out from 2005 and forward.

The SA for the [^{11}C]CH_4 target has fluctuated during the time of this study, the major trend being that it increases over time. However, we also experienced a drop in SA in the first half of the year 2006 (discussed below). Thirteen of the sixteen batches included for [^{11}C]FLB 457 were produced in 2004, and similarly six of eight batches for [^{11}C]PE2I were produced in the first half of 2006, explaining why the mean SA for these two radioligands are not as high as expected.

In addition, a limited literature search was performed on reported values of SA for carbon-11 methylations. In the search we found six articles from four different groups, all articles described radiopharmaceuticals produced from [^{11}C]CO_2[95-100]. The reported SA ranged from 56 to 222 GBq/μmol at EOB for five of the articles, which is very much in line with the SA from our in-house [^{11}C]CO_2 production reported in Table 2. However, Ermert and co-workers[100] reported six productions from [^{11}C]CO_2 with SA ranging from 111 to 15 876 GBq/μmol at EOB. This was performed using ”wet” ($LiAlH_4$/Ph_3PI_2) chemistry, and required thorough flushing of the chemistry system overnight as well as at least three pre-irradiations on the target. Their results provide evidence that very high SA is possible to reach also with the use of target produced [^{11}C]CO_2. However, cumbersome precautions need to be adhered before each production, whereas the method reported here needs no pre-irradiations on the target and only 10 – 20 minutes flushing with helium through the recirculation system.

The deviation of the measured SA was large (Table 2). The high deviation could have occurred during three steps: (i) during the actual [^{11}C]CH_4 production in the target (ii) during the conversion of [^{11}C]CH_4 to the final radiolabeled tracer or (iii) during the SA measurements. The high deviations indicate that we did not succeed in reaching as high SA for every production as we would hope for. Also, the inherent fault in SA measurements using UV detection does increase with increasing SA, as the low concentrations we are measuring for the higher SA gives lower signal to noise ratio. Improved analytical techniques such as fluorescence detection may improve the deviation of the SA measurements in this case. However, there was a high standard deviation also for radioligand productions with low SA from the [^{11}C]CO_2 target (Table 2).

The SA increased after repeated irradiations on the [^{11}C]CH_4 target (Figure 6). Irradiations on the target reduce the cold carbon contaminations, which most likely is why we saw increasing SA over time. For all radiotracers produced by methylations starting from [^{11}C]CH_4, a dip in SA in the first half of the year 2006 was observed. We have been able to correlate that to a decreased flow of the gas from the target. These productions are not methylations and are not included in this study, but somehow the flow seems to have an effect on the SA also for the methylations. The flow from the target to the methylation system was over 400 ml/min, but for other synthesis (i.e. ^{11}C-cyanations) we used 200 ml/min, with no flushing of the target between the ^{11}C-cyanation and ^{11}C-methylation productions.

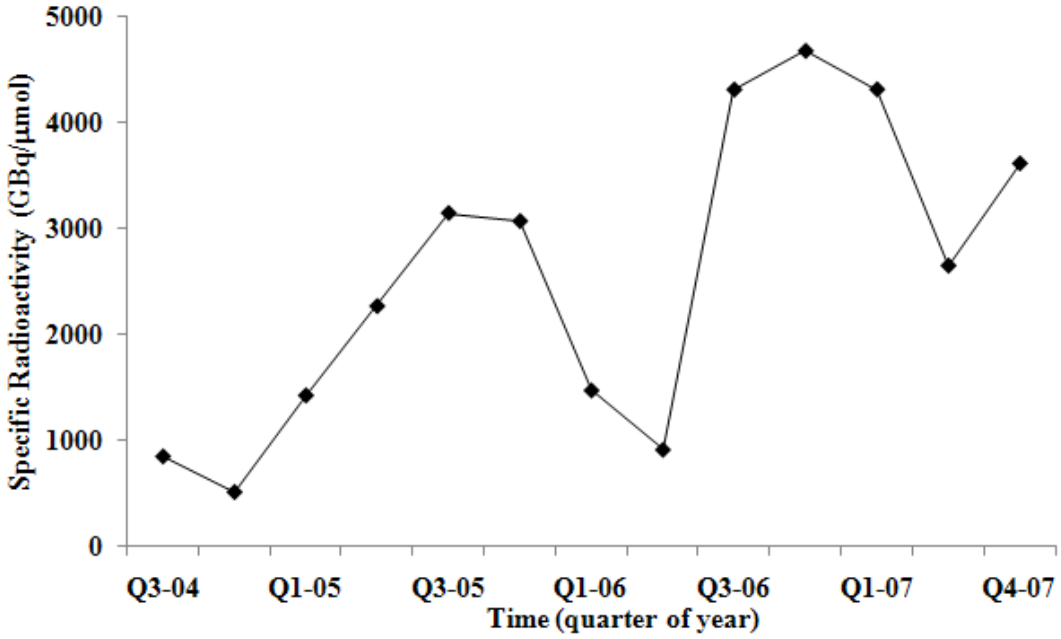

Figure 6. Specific radioactivity (SA) over time of [^{11}C]raclopride when synthesized from [^{11}C]CH_4 produced *in situ* in the target. Time is divided into quarters of a year (Q1, Q2 etc.). Specific radioactivity (SA) is given as the mean value in GBq/µmol at the end of bombardment (EOB); No productions of [^{11}C]raclopride was performed during Q2-2007.

While the standard deviation of the measured SA was large, the SA increased with time. As a result the minimum SA measured for the last 52 productions of [^{11}C]raclopride was 967 GBq/µmol which still is higher than any production from the [^{11}C]CO_2 target. In addition this SA would be sufficient to assure less than 5% occupancy also for high affinity PET radioligands such as [^{11}C]FLB 457[39].

4.2 RADIOLIGANDS SYNTHESIZED FROM [^{11}C]HCN (PAPER II AND III)

After the positive results of SA improvement when using in-target produced [^{11}C]CH_4 for ^{11}C-methylations, a system for ^{11}C-cyanations was set up. Two different radiotracers were produced and the SA was compared when ^{11}C-cyanation labelings were performed starting from in-target produced [^{11}C]CO_2 (one radiotracer) and [^{11}C]CH_4 (two radiotracers).

4.2.1 Radiochemistry

For the ^{11}C-cyanation of aryl-bromide precursors, two synthetic strategies were considered, ^{11}C-cyanation via the traditional copper catalyzed Rosenmund-von Braun reaction[101] or via the palladium catalyzed reaction[102]. We decided to utilize the palladium catalyzed approach in radiosynthesis, because in the synthesis of [^{11}C](Z,Z)-BABCH Siméon et al.[103] reported a comparison of copper catalyzed and palladium catalyzed ^{11}C-cyanations and in their labelling conditions, they found the palladium catalyzed reaction more efficient.

[^{11}C]HCN is produced by letting [^{11}C]CH_4 and NH_3 pass over platinum catalyst at high temperature. NH_3 concentration is very important for the [^{11}C]HCN formation, and in our system 10-15 vol % was found to be sufficient. A furnace temperature of 990°C gave significantly better conversion (42 ± 17%, n = 3) than a temperature of 950°C (11 ± 2%, n = 2), which is not in accordance to previously published data[27]. The

over-all conversion yields were lower than what has been previously reported. Explanations for the low yields could be the contact time for the gas with platinum, or possibly the low platinum amount we used (1.3 g instead of 3 g)[27]. Another possible reason is that oxygen or H_2O is interfering with the catalytic reaction of [^{11}C]CH_4 with NH_3 on Pt. Iwata et al[27] reported the effect of absorbers to improve the yield, achieving close to quantitative conversion when metallic sodium coated on quarts wool was used.

Two radiotracers were labelled using [^{11}C]HCN; [^{11}C]Ximelagatran and [^{11}C]AR-P135003 (Scheme 2). Precursors and reference standards were obtained in collaboration with AstraZeneca R&D Mölndal and Södertälje, Sweden. The labelling reactions provided ^{11}CN-incorporations with good yield for both compounds, with only small variation between synthesis repetitions (between 70% and 80%).

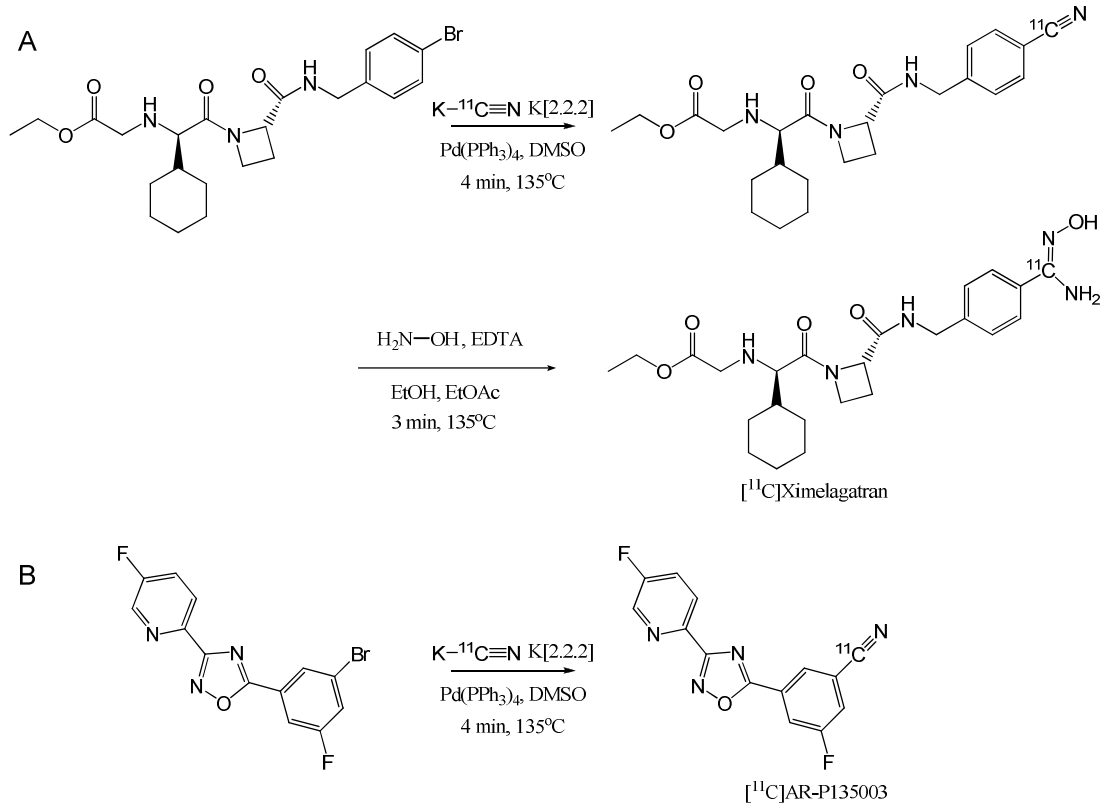

Scheme 2. Synthesis of A) [^{11}C]Ximelegatran and B) [^{11}C]AR-P135003.

To afford the hydroxyamidine [^{11}C]Ximelagatran, the labeled nitrile was treated with hydroxylamine. The reaction was completed in 3 minutes in a mixture of EtOH and EtOAc in a presence of small amount of EDTA (Scheme 2A). This is in contrast to classical chemistry, where the reaction between the nitrile and hydroxylamine can take several hours to days[104, 105].

4.2.2 Specific radioactivity

Specific radioactivity of the radioligands produced from [^{11}C]HCN was about nine times higher when produced from in-target produced [^{11}C]CH_4 than [^{11}C]CO_2 (Table 3). The finding that the SA was higher for the productions using in-target produced [^{11}C]CH_4 was in line with our observations from the ^{11}C-methylation reactions. However, the SA in the syntheses using [^{11}C]HCN were consistently lower compared to the productions from [^{11}C]CH_3I. This indicates that isotopic dilution occurred during the Pt catalyzed conversion of [^{11}C]CH_4 to [^{11}C]HCN. From in-target

produced [^{11}C]CH_4 the final formulations of ^{11}C-cyanations contained a mean quantity of cold compound of 16 nmol and for ^{11}C-methylations the quantity at the same time was 0.7 nmol. The irradiation process was kept the same (35μA, 20 min) and the mean radioactivities in the final formulations were similar; for the ^{11}C-cyanations (961 MBq) and the ^{11}C-methylations (922 MBq). The same comparison from the [^{11}C]CO_2 target gives 75 nmol for the ^{11}C-cyanations (mean radioactivity of 553 MBq) and 31 nmol for ^{11}C-methylations (mean radioactivity of 825 MBq), however in this case the irradiation process varied more as did the final radioactivities making a direct comparison challenging.

Table 3. Specific radioactivity of [^{11}C]AR-P135003 and [^{11}C]Ximelagatran

Target	[^{11}C]CO_2	[^{11}C]CH_4	
Radioligand	[^{11}C]AR-P135003	[^{11}C]AR-P135003	[^{11}C]Ximelagatran
SA (GBq/mmol)	44	398	406
n	10	41	3
min (GBq/mmol)	18	67	375
max (GBq/mmol)	115	894	430
A (MBq)	553	903	1754
m (nmole)	75	16	20

SA at EOB, n = number of productions, Min and Max are the lowest and highest measured SA respectively, A = Radioactivity in final formulation, m = mean amount of the cold compound in the final formulation.

Flushing with helium gas through the heated oven for 30 minutes before radioactivity takedown was found to increase the SA, which indicates that the isotopic dilution was due to trapped CH_4 or HCN on the Pt catalyst. Another possible source could be contaminants in the ammonia gas.

4.3 MGLUR5 PET RADIOLIGAND DEVELOPMENT (PAPER III)

One of the radioligands labeled using the secondary labeling precursor [^{11}C]HCN was the potential mGluR5 radioligand [^{11}C]AR-P135003. The aryl bromide precursor was obtained with the co-operation of AstraZeneca LTD, Södertälje, Sweden. *In vivo* characterization of [^{11}C]AR-P135003 was performed including seven PET measurements in three cynomolgus monkeys. [^{11}C]AR-P135003 showed high uptake in regions known to contain mGluR5 (Figure 7).

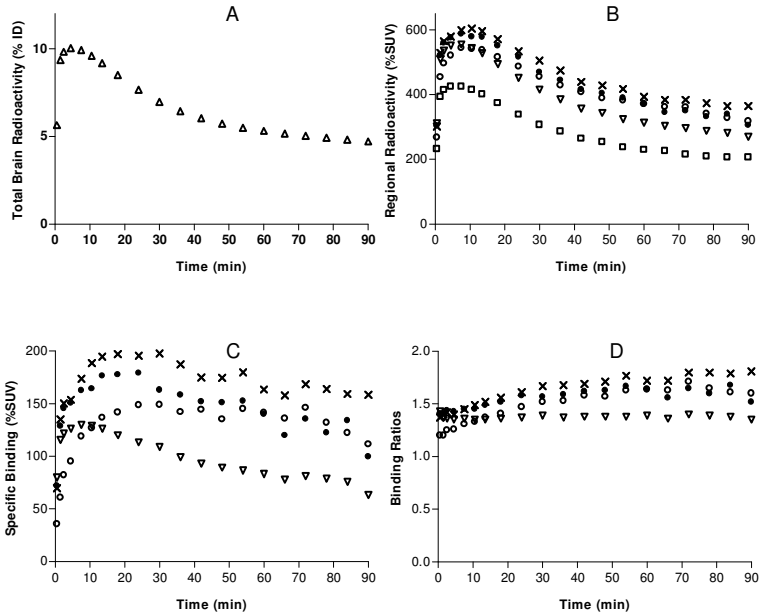

Figure 7. Mean time course for radioactivity in the brain of cynomolgus monkeys (n=5) after i.v. administration of [^{11}C]AR-P135003 during baseline measurements. A) Total brain uptake. B) Regional radioactivity. C) Specific binding. D) Binding ratios. Key: Δ Whole brain; × Caudate; • Cingulate Gyrus; o Thalamus; ∇ Temporal Cortex; □ Cerebellum.

Co-injection with the cold compound distinctly decreased regional radioactivity of [^{11}C]AR-P135003 in mGluR5 rich regions in a dose-dependent fashion (Figure 8).

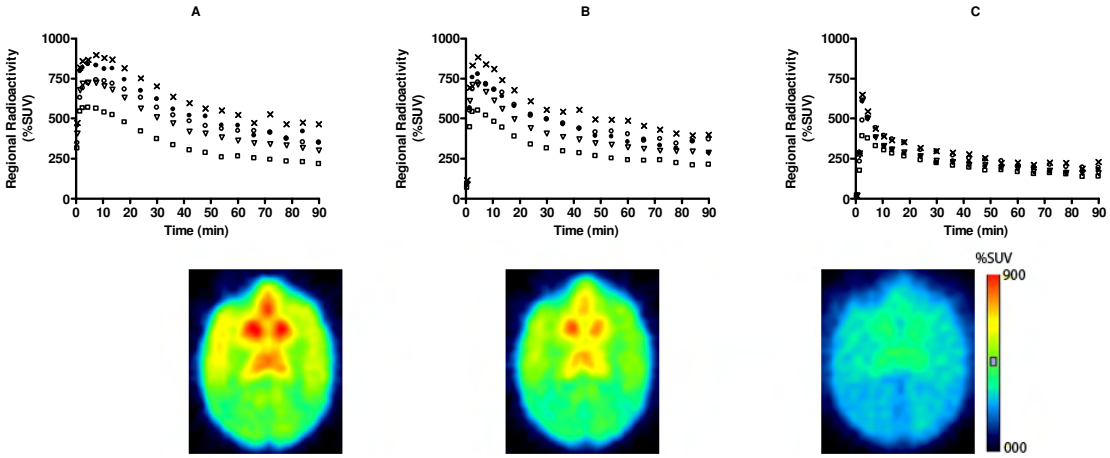

Figure 8. Time curves and summation images (6 to 93 minutes) showing regional distribution of radioactivity in the brain of a cynomolgus monkey after i.v. administration of [^{11}C]AR-P135003 during A) Baseline condition, B) After co-injection of 0.04 mg/kg of AR-P135003 and C) After co-injection of 0.4 mg/kg of AR-P135003. Key: × Caudate; • Cingulate Gyrus; o Thalamus; ∇ Temporal Cortex; □ Cerebellum.

Analysis of radiometabolites measured in cynomolgus monkey plasma was performed using HPLC. The injected radioactivity eluted from HPLC within 6-7 minutes. The metabolism was relatively slow with an amount of the total radioactivity in plasma representing unchanged radioligand was 96%, 83% and 72% at 4, 15 and 30 minutes respectively. All radiolabeled metabolites were more hydrophilic than the mother compound based on the elution from the HPLC.

This first characterization showed that [^{11}C]AR-P135003 enter the brain to a high extent, the binding was saturable and the regional radioactivity pattern was in accordance with the known distribution of mGluR5.

4.4 β-AMYLOID PET RADIOLIGAND DEVELOPMENT (PAPER IV)

β-amyloid accumulation is associated with the pathogenesis of Alzheimer's disease (AD). Among the PET radioligands that have been investigated for visualization of amyloid plaques to date, [^{11}C]PIB is the most extensively studied. Although PET imaging with [^{11}C]PIB has provided valuable new information, the high degree of white matter retention displayed by [^{11}C]PIB may limit its use as a tool for early diagnosis of AD when plaque levels are low.

AZD2184 has recently been proposed as a new radioligand for high contrast imaging of Aβ–deposits after characterization on human amyloid fibrils *in vitro* and in rodents *ex vivo*[62].

4.4.1 Radiochemistry

Precursors and reference standards were obtained in collaboration with AstraZeneca R&D Södertälje, Sweden. Due to the similarity between the chemical structures of [^{11}C]AZD2184 and [^{11}C]PIB (Figure 2), the obvious starting point in radiolabeling was the direct methylation using [^{11}C]CH_3OTf, without any added base at 80 °C. However, this route yielded no labeling product. Addition of aqueous base resulted in only *O*-methylation, which was anticipated since the alkoxide group is a stronger nucleophile than the amino group at such basic conditions. In the last effort with the unprotected precursor we tried a weaker base (tetramethylpiperidine, TMP), however only very low incorporation yields could be obtained (less than 2%).

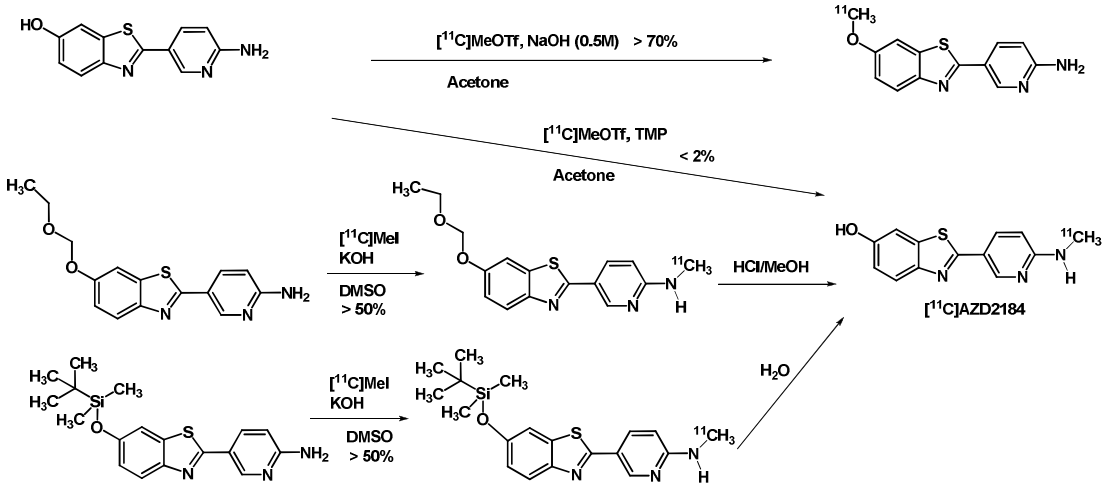

Scheme 3. Radiosynthesis of [^{11}C]AZD2184.

The next step was to utilize protection on the phenol to allow for more basic conditions in the labeling. Protection with an ethoxymethoxy group and a *tert*-butyldimethylsilyl group was tried and labelings were performed with methyl iodide in DMSO at 125 °C. Both methods were successful with incorporation yields over 50% and quantitative deprotection. The *tert*-butyldimethylsilyl group is usually removed by acids or fluoride ions[106], but we incidentally realized that adding a small amount of water to the basic reaction mixture was enough for successful deprotection in this case

(Scheme 3). This easy deprotection made us choose the *tert*-butyldimethylsilyl protected precursor for all productions for PET. The total overall decay corrected yield starting from [^{11}C]CH_4 was 4-13% (n=5) with a total synthesis time of 30-33 minutes, and the range of specific radioactivity was 1600-4000 GBq/μmol at end of synthesis. Radiochemical purity after HPLC purification exceeded 99% for all productions.

4.4.2 Brain PET measurements

Following injection of [^{11}C]AZD2184 in cynomolgus monkey, a reasonable amount (2.2% to 3.4% of injected dose) of radioactivity entered the brain. The distribution was fairly uniform and showed a rapid washout in all regions (Figure 9).

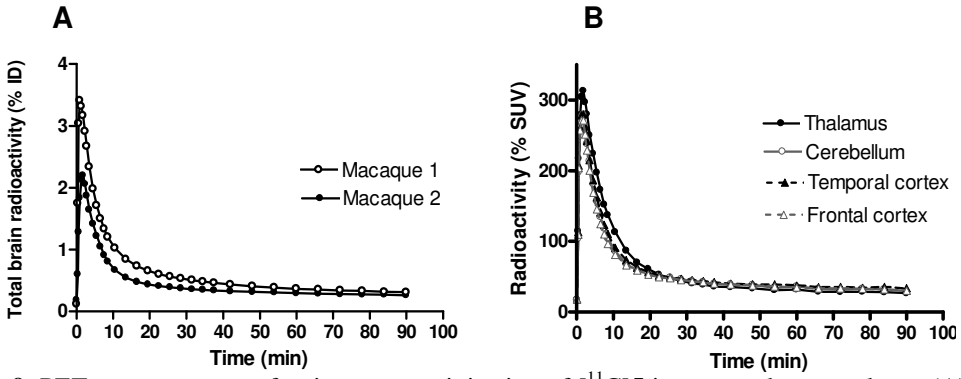

Figure 9. PET measurements after intravenous injection of [^{11}C]**5** in cynomolgus monkeys. (A) Total brain radioactivity presented as percentage of injected dose (ID) in two monkeys. Data represent mean values from two measurements. (B) Time curves of regional brain radioactivity presented as percent standardized uptake value (SUV). Data represent mean values from two measurements in the two monkeys.

The studies were performed in cynomolgus monkeys that were assumed to be virtually free from amyloid plaques. Compared to [^{11}C]PIB, [^{11}C]AZD2184 showed signs of less white matter binding. The washout was fast for [^{11}C]AZD2184 and the ratio between radioactivity at peak uptake and at a late time point (60 minutes) is significantly higher for [^{11}C]AZD2184 (8.2) than what has been published for [^{11}C]PIB (4.6)[107]. Also the uniform distribution, with no difference in binding between regions rich in white matter to those containing less white matter is in contrast to [^{11}C]PIB measurements and indicates low white matter binding of [^{11}C]AZD2184.

4.4.3 Whole body PET measurements

A preliminary whole body dosimetry measurement was performed with [^{11}C]AZD2184 in a single cynomolgus monkey using a Siemens Biograph 64 PET system. The obtained organ curves were entered into the OLINDA software (Vanderbilt University, Nashville, TN), which is an FDA-approved tool for performing organ level internal dose calculations. The software generates Effective Dose (ED) estimates in the unit of μSv/MBq, based on adult human male and female organ models. The organ with the highest radiation burden was the urinary bladder wall (49.7 μSv/MBq) followed by the small intestines (30.3 μSv/MBq) and the gallbladder (23.4 μSv/MBq).

Effective dose estimates is considered the most accurate measure of radiation risks[108]. For [^{11}C]**5**, the estimated effective dose was 6.2 μSv/MBq for an adult male, which is similar to other ^{11}C-labeled compounds including [^{11}C]PIB (4.7 μSV/MBq)[109]. The European commission guidelines states a maximum limit of 10 mSv per year[110]

and subject, so this preliminary dosimetry measurement gives an indication that multiple scans in one year in the same subject would not be a problem from a radiation stand point. This may be an advantage when comparing different amyloid imaging probes and enables plaque imaging and [^{18}F]FDG measurement of cerebral metabolism on the same day. Also the shorter half-life leads to less radiation burden for the patient. This is of particular advantage in investigations where a longitudinal design is desired, such as studies to follow disease progression or the outcome of treatment with a disease modifying drug. However, the short half-life of carbon-11 limits the use of [^{11}C]AZD2184 to PET centers with a cyclotron. Thus, the development of a fluorine-18 labeled derivative of [^{11}C]AZD2184 would extend the availability of the radioligand.

4.4.4 Radiometabolites in plasma

Metabolism of [^{11}C]AZD2184 was fast. Less than 10% of the unchanged radioligand remained fifteen minutes after administration.

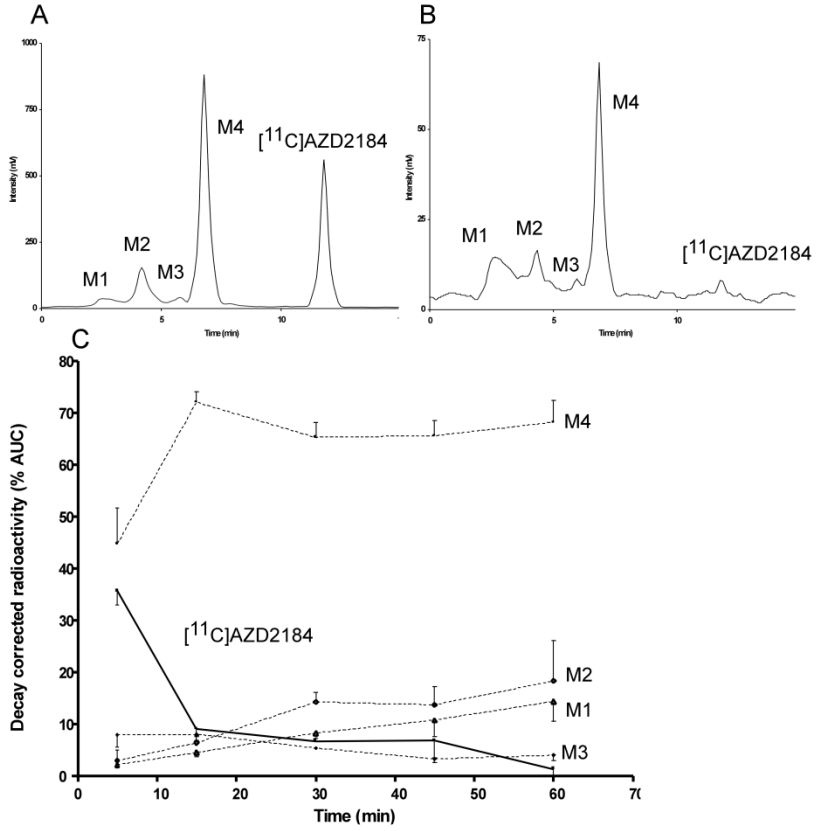

Figure 10. HPLC Analysis of metabolites in cynomolgus monkey. (A) Radiochromatogram of the metabolism at 5 minutes after [^{11}C]**5** administration. (B) Radiochromatogram of the metabolism at 45 minutes after [^{11}C]**5** administration. (C) Percentage of total radioactivity of unmetabolised [^{11}C]**5** as well as the percentages of the metabolites. Sampling times were 5, 15, 30 and 45 minutes. Graph shows the mean with single direction bars presenting the standard deviation. N = 4 for the 5, 15 and 45 minutes and N = 3 for the 30 minute time point.

Four metabolites could be seen on HPLC and all were more hydrophilic than the mother compound (Figure 10). For [^{11}C]PIB, more than 95% of the radioactivity in mice brain has been shown to be from the unmetabolized species[107]. The fact that the rate of metabolism of [^{11}C]AZD2184 is similar to that reported for [^{11}C]PIB and the similarities in structure between the compounds, gives us no reason to believe that radiometabolites of [^{11}C]AZD2184 enter the brain to any great extent.

4.5 5-HT$_{1B}$ PET RADIOLIGAND DEVELOPMENT (PAPER V AND VI)

The 5-HT$_{1B}$ receptor is implicated in a number of serotonin related psychological disorders and is therefore a very interesting target to visualize with molecular imaging techniques such as PET. Before the start of this thesis work there was no available PET radioligand for the visualization of the 5-HT$_{1B}$ receptor.

4.5.1 Eight carboxamide radioligands (Paper V)

In collaboration with AstraZeneca Pharmaceuticals LP (Wilmington, DE, USA) we searched in their compound library to find compounds with attributes that would fit a 5-HT$_{1B}$ PET radioligand. The target PET radioligand profile consisted of: high affinity (Ki = 0.1 – 0.5 nM), good selectivity over other receptor proteins (at least 100 fold, 10 times over 5-HT$_{1D}$), moderate lipophilicity (logD around 1.5) and it should not be an efflux substrate. Eight candidate compounds (Figure 11, pharmacological characteristics given in Table 4) were selected for labeling with carbon-11, initial PET measurements in cynomolgus monkeys and radiometabolite analysis.

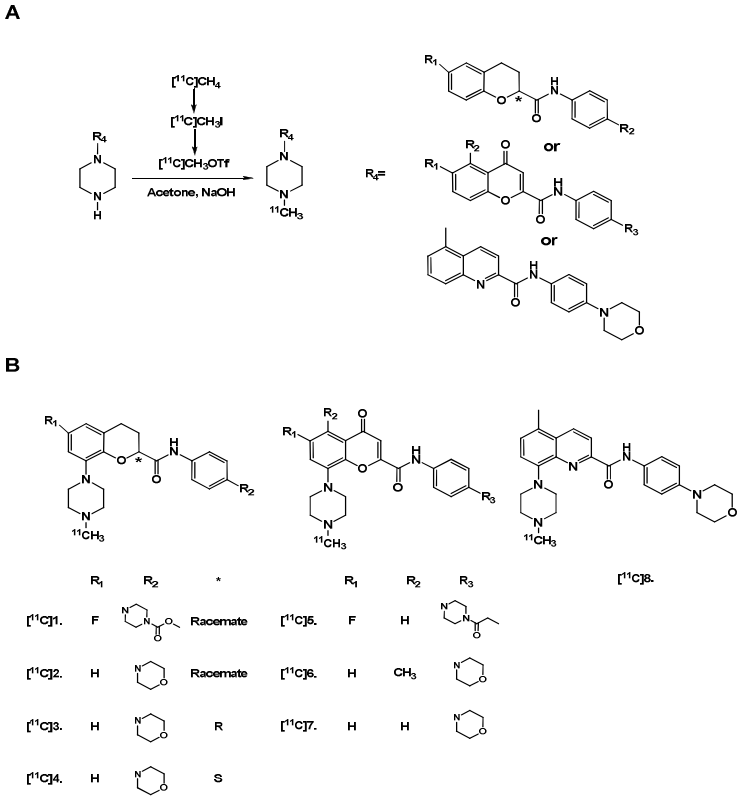

Figure 11. (A) Carbon-11 labeling of eight potential 5-HT$_{1B}$ radioligands. (B) Structures of the eight compounds divided into three different core structures.

Carbon-11 labelings of compounds **1-8** were based on *N*-alkylation on a secondary amine group using [^{11}C]CH$_3$OTf in acetone with NaOH as the base (Figure 11).

Table 4. Pharmacological characteristics of the compounds investigated in this report.

Compound	MW (g/mol)	cLogD (pH = 7.4)	cLogP	Binding affinity (5-HT1B, Ki, nM)	Binding affinity (5HT1A, Ki, nM)	Selectivity (5-HT1A)	Agonism (EC50, nM)	Antagonism (IC50, nM)	Efflux ratio (BA/AB)
1	512	0.90	1.51	0.5	247	490	8.0E-10	>2.5e-7	1.1
2	437	1.39	2.01	0.4	34	85	<3.5E-10	2.1E-10	1.6
3	437	1.39	2.01	0.3	52	150	4.9E-10	nm	2.1
4	437	1.39	2.01	0.6	34	55	9.7E-10	nm	nm
5	522	1.25	1.88	2	>2570	>1300	>5.0E-6	3.5E-9	3.8
6	463	1.26	1.90	0.6	49	80	nm	5.0E-8	1.2
7	449	0.76	1.39	0.2	71	350	<5.2E-9	8.8E-9	1.1
8	446	1.70	2.35	0.2	40	270	<3.0E-9	>1.2e-6	0.3

LogD and LogP values were calculated using Pallas 3.0 (CompuDrug Chemistry Ltd.), nm = not measured.

Target produced [^{11}C]CH_4 was utilized for the production of [^{11}C]CH_3OTf in all the preparations of radioligands in this study. This helped us achieving a mean specific radioactivity (SA) of 299 GBq/µmol (8075 Ci/mmol, n=12) at the time of administration, and thus ensuring tracer dose conditions in the PET measurements for all radioligands.

4.5.2 PET in non-human primates

Seven of the eight radioligands showed reasonably good brain uptake and the brain uptake correlated with the lipophilicity of the compounds (Figure 12).

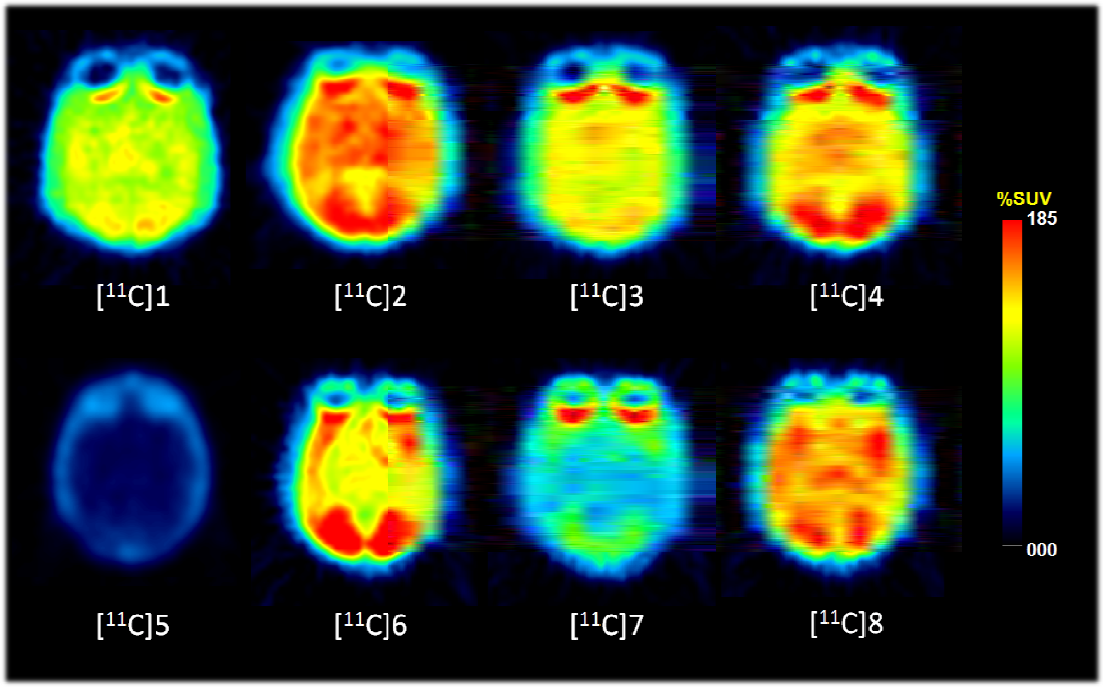

Figure 12. Summation PET images showing radioactivity distribution for eight radioligands in a horizontal section of the cynomolgus monkey brain. The images represent integrated radioactivity from 9 to 93 minutes after radioligand injection.

The only notable exception was [^{11}C]**8** that despite high lipophilicity compared to the other radioligands only entered the brain to moderate extent. The higher lipophilicity of [^{11}C]**8** may lead to low plasma solubility, lung and liver uptake as well as non-specific binding to plasma proteins that reduces the free fraction and subsequently lower the brain uptake[15]. It should however be noted that the cLogP for [^{11}C]**8** is 2.35 which is well in the range for optimum LogP values (2.0 – 3.5) reported for many drug classes.

[^{11}C]**5** only entered the brain in low amount, most likely due to it being a substrate for efflux proteins (Table 4, an efflux ratio >3 might indicate this). The unlabelled **5** has successfully been used as a blocker in *in vivo* studies in guinea pigs[111], indicating reasonable brain exposure. This discrepancy can either be due to species differences between guinea pig and cynomolgus monkey or be an effect of the higher dose given in the guinea pig studies. A higher dose can saturate e.g. the efflux proteins or specific or non-specific binding on plasma proteins leading to higher brain penetration of the drug[15].

Five of the seven radioligands with reasonable brain uptake, showed a heterogeneous distribution within the brain (Figure 13), in accordance with the known distribution of 5-HT$_{1B}$ receptors. [^{11}C]**8** showed homogenous distribution, indicating higher non-specific binding of that radioligand, likely due to the higher lipophilicity.

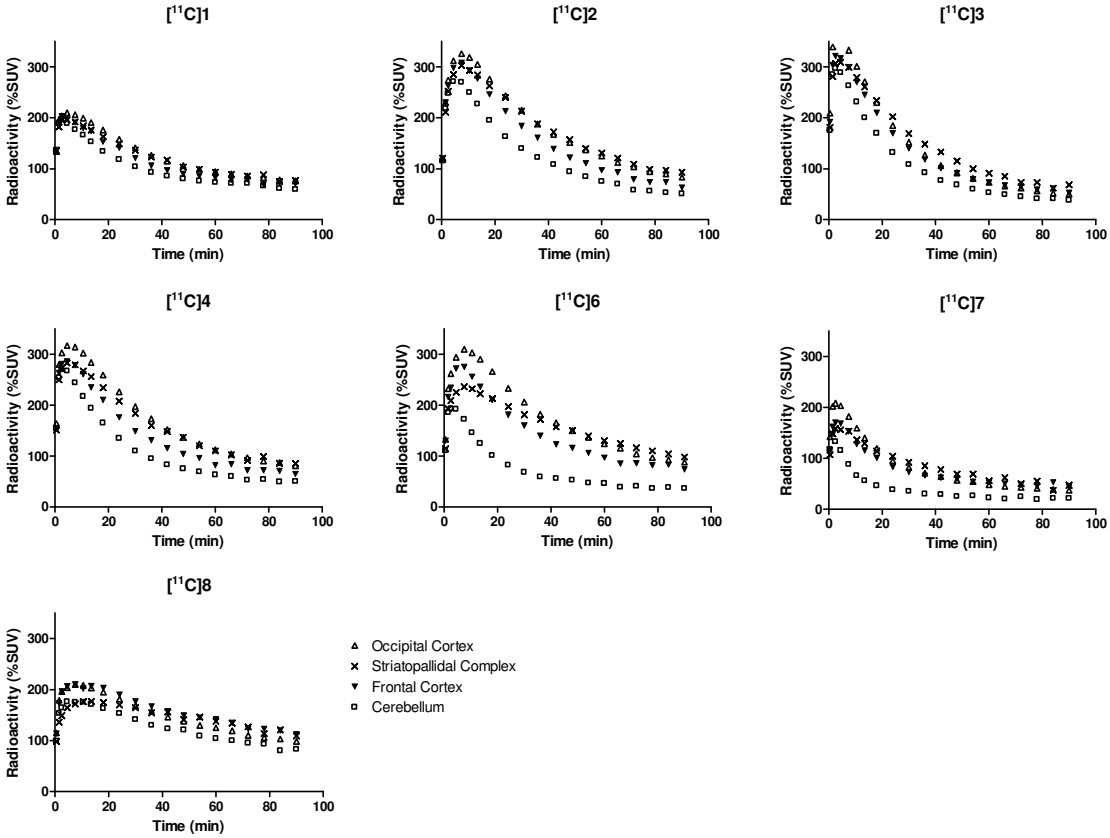

Figure 13. Time activity curves for regional brain uptake in the occipital cortex, striatopallidal complex, frontal cortex and cerebellum after iv administration of radioligand in cynomolgus monkey.

The cerebellum is a region with low density of 5-HT$_{1B}$ receptors[74] and was used as a reference region for non-specific and non-displaceable binding. There was a positive correlation between the relative lipophilicity and non-specific binding of the compounds (Figure 14), a relationship which is in line with previous studies in series of other chemical structures[107].

In an attempt to draw general conclusions on the relationship between the physicochemical properties of compounds and the effect this imposes in the *in vivo* setting, we could see a quadratic correlation between the lipophilicity of the compounds and the peak in whole brain uptake (Figure 14A) which is in line with other studies[15]. The correlation might have been clearer if additional radioligands with higher lipophilicities would have been included. Leaving [^{11}C]**8** out of the fit and looking only

at the more hydrophilic radioligands, a linear relationship can be detected (R^2 = 0.8). Also the non-specific binding, shown as the radioactivity in cerebellum at 60 minutes post administration, is positively correlated with the lipophilicity (Figure 14B). This can in part be due to the higher initial uptake shown in Figure 14A, however [^{11}C]**8** still had higher non-specific binding even though the initial uptake was lower than for other compounds. Interestingly, relatively high non-specific binding was found for [^{11}C]**1** despite low lipophilicity and relatively low initial uptake.

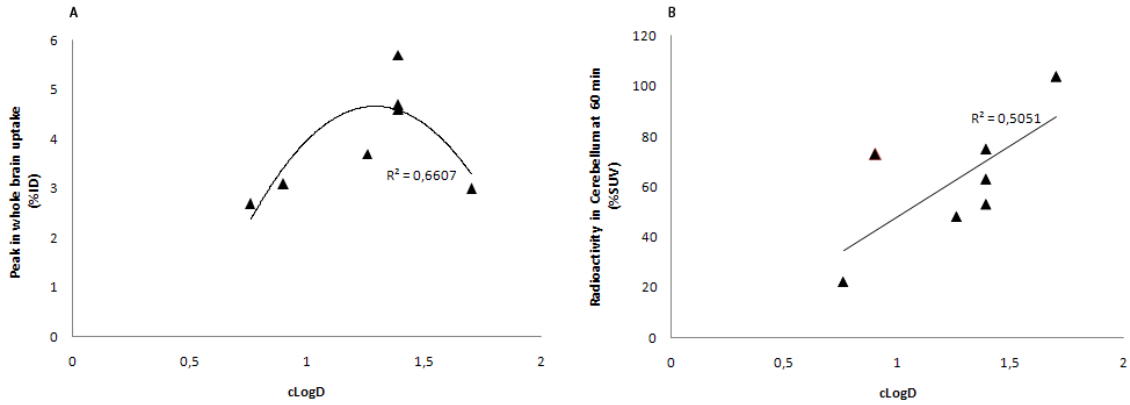

Figure 14. A. Peak in whole brain uptake and B. Radioactivity in cerebellum at 60 minutes plotted against the lipophilicity for the eight radioligands.

Time activity curves were generated for specific binding which thus was estimated as radioactivity in the region of interest minus radioactivity in the cerebellum. Cerebellum was also used to calculate binding ratios (radioactivity in a region of interest divided by radioactivity in the cerebellum). Time activity curves for the three radioligands with the best binding profile (good brain uptake in 5-HT_{1B} rich regions and low cerebellar binding) [^{11}C]**4**, [^{11}C]**6** and [^{11}C]**7** are shown in figure 15. The specific binding curves were higher for [^{11}C]**6** than for any other compound with a peak above 150% SUV at 20 minutes for the occipital cortex and ratios reaching 3.0 for the occipital cortex and striatopallidal complex. [^{11}C]**7** also shows ratios of 3.0 for the occipital cortex, however the fast kinetics results in a specific binding peak equilibrium time of only 7 – 10 minutes. A too early peak in specific binding might result in a problematic quantification due to the contribution of blood flow. However, it cannot be ruled out that the peak of specific binding for [^{11}C]**7** might arise later in human applications as observed for [^{11}C]**6** (see below).

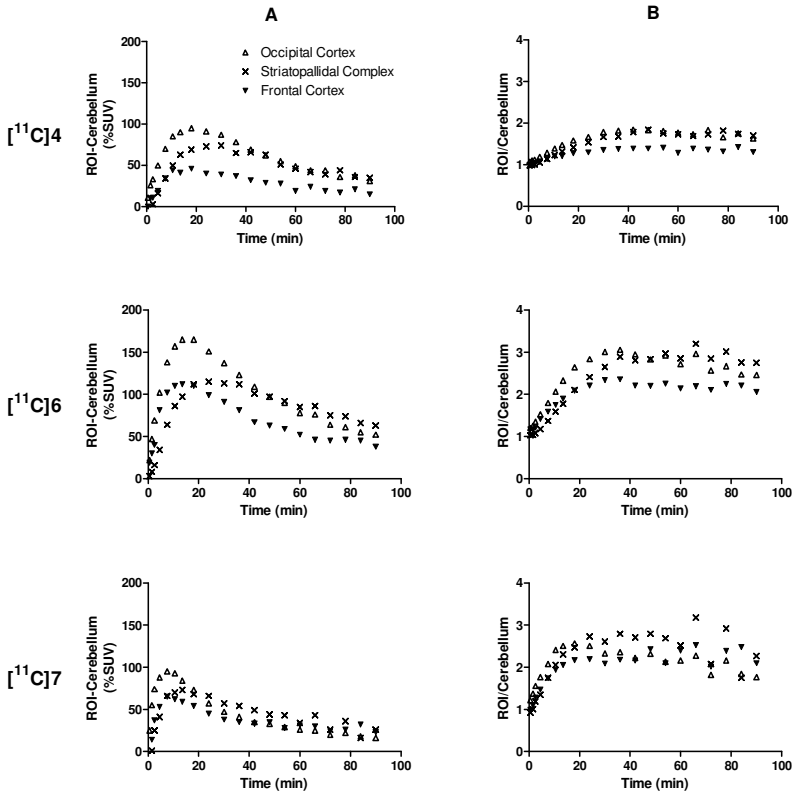

Figure 15. Time curves after iv administration of radioligands [^{11}C]**4**, [^{11}C]**6** and [^{11}C]**7** in cynomolgus monkey. (A) Specific binding in each of the target regions using cerebellum as reference region for non-displaceable binding. (B) Ratios of radioactivity in each of the target regions to radioactivity in the cerebellum.

As indicated by the binding ratios, also the binding potentials (BP_{ND}) calculated using the SRTM were higher for [^{11}C]**6** and [^{11}C]**7** than for any of the remaining radioligands (Table 5).

Table 5. Binding potentials (BP_{ND}) in occipital cortex, striatopallidal complex and frontal cortex.

Monkey (weight)	1 (3.1 kg)			2 (3.4 kg)		3 (4.3 kg)			4 (6.8 kg)
Radioligand	[^{11}C]1	[^{11}C]3	[^{11}C]4	[^{11}C]2	[^{11}C]6	[^{11}C]6	[^{11}C]7	[^{11}C]8	[^{11}C]6
Brain Region									
Occipital Cortex	0.28	0.34	0.62	0.48	1.28	1.52	1.17	0.19	1.27
Striatopallidal Complex	0.25	0.46	0.55	0.51	1.14	1.44	1.29	0.28	1.79
Frontal Cortex	0.13	0.26	0.29	0.26	0.71	1.01	0.98	0.35	0.81

Binding potentials were calculated using the single reference tissue model (SRTM) with cerebellum as the reference region.

Radiometabolites of the radioligands measured in monkey plasma were analyzed by HPLC. The chroman radioligands ([^{11}C]**1**, [^{11}C]**2**, [^{11}C]**3** and [^{11}C]**4**) were faster metabolized than the chromenone ([^{11}C]**5**, [^{11}C]**6** and [^{11}C]**7**) as well as the quinoline ([^{11}C]**8**) radioligands. The amount of unchanged radioligand was 86 – 97% and 15 – 69% at 5 and 30 minutes, respectively (Table 6). All metabolites were less lipophilic than their mother compounds based on the order of elution from the HPLC. The general pattern of radiometabolism showed by HPLC was one or two hydrophilic metabolites and the pattern was shared among all eight radioligands.

Table 6. Radiometabolism measured in cynomolgus monkey plasma using HPLC.

Radioligand	[^{11}C]1	[^{11}C]2	[^{11}C]3	[^{11}C]4	[^{11}C]5	[^{11}C]6	[^{11}C]7	[^{11}C]8
Sampling Time (min)	% Unchanged Radioligand							
5	94	97	86	90	85	91	nm	89
30	50	38	15	29	69	67	69	72

nm = not measured.

One might consider that the relative washout for the racemate and separated enantiomers, where the washout of [^{11}C]**3** > [^{11}C]**4** > [^{11}C]**2**, can be due to the relative speed of metabolism. Faster peripheral metabolism would lead to lower concentration of the unchanged radioligand in blood, and thus a gradient being created between the blood and brain compartments with a faster washout from brain as result.

4.5.3 Further characterization of [^{11}C]AZ10419369 (Paper VI)

From the extensive evaluation described in the previous section, [^{11}C]**6** ([11C]AZ10419369) was found to be the most promising radioligand for PET imaging of 5-HT$_{1B}$ receptors, and was thus selected for further characterization.

The specificity of [^{11}C]AZ10419369 binding to the 5-HT$_{1B}$ receptor *in vivo* was supported by a dose-dependent reduction in brain regional radioactivity by pretreatment with the reference 5-HT$_{1B}$ antagonist AR-A000002 in cynomolgus monkeys (Figure 16). The radioactivity in regions known to contain 5-HT$_{1B}$ receptors was markedly reduced. This observation confirms that a large portion of [^{11}C]AZ10419369 binding represents specific binding to the 5-HT$_{1B}$ receptor.

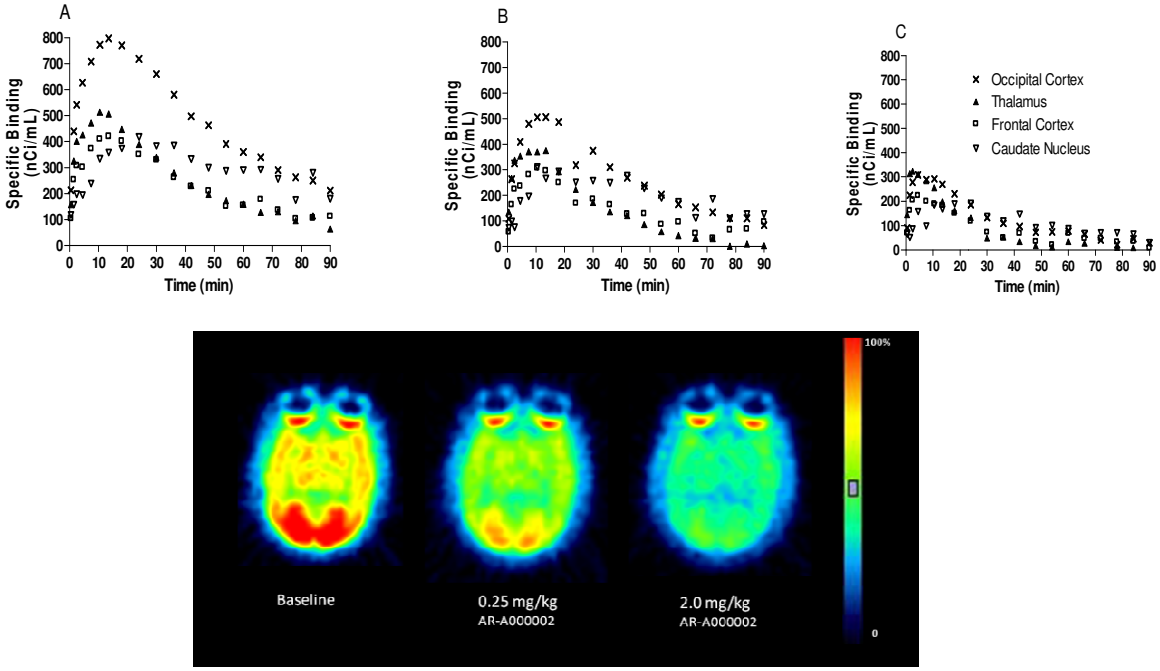

Figure 16. Time curves for regional radioactivity and summation images from 9-93 minutes showing the distribution of radioactivity in the cynomolgus monkey brain after iv injection of [^{11}C]AZ10419369 during A) Baseline condition, B) Preatreatment with 0.25 mg/kg AR-A000002 and C) Preatreatment with 2.0 mg/kg AR-A000002.

To provide more detailed information on the regional distribution of AZ10419369 binding, the compound was labeled with tritium for autoradiographic

studies in the cynomolgus monkey brain. The distribution pattern of [^{3}H]AZ10419369, characterized by high densities in the ventral striatum and pallidum, globus pallidus, visual cortex, and substantia nigra, is in close agreement with the regional distribution seen in the present PET study as well as with previous reports describing the regional brain distribution of 5-HT$_{1B}$ receptors[73, 74].

Preliminary PET-measurements (Figure 17) in human subjects confirmed high brain exposure of [^{11}C]AZ10419369 and a regional brain distribution consistent with that seen in monkeys *in vivo* as well as *in vitro*. Time curves for specific binding indicated that equilibrium was reached during the PET measurement for cortical regions, thalamus and dorsal striatum (Figure 18) but in most cases not for globus pallidus.

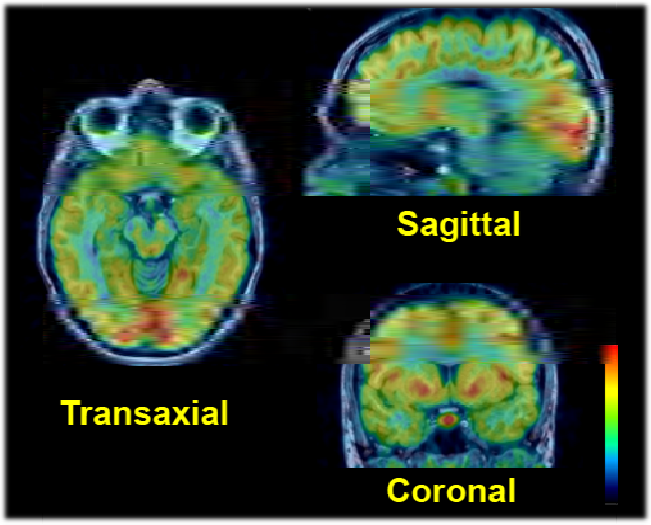

Figure 17. Fused PET-MRI images of [^{11}C]AZ10419369 regional brain uptake in a human subject. Images were obtained by summation of the frames from 3-93 minutes after intravenous injection.

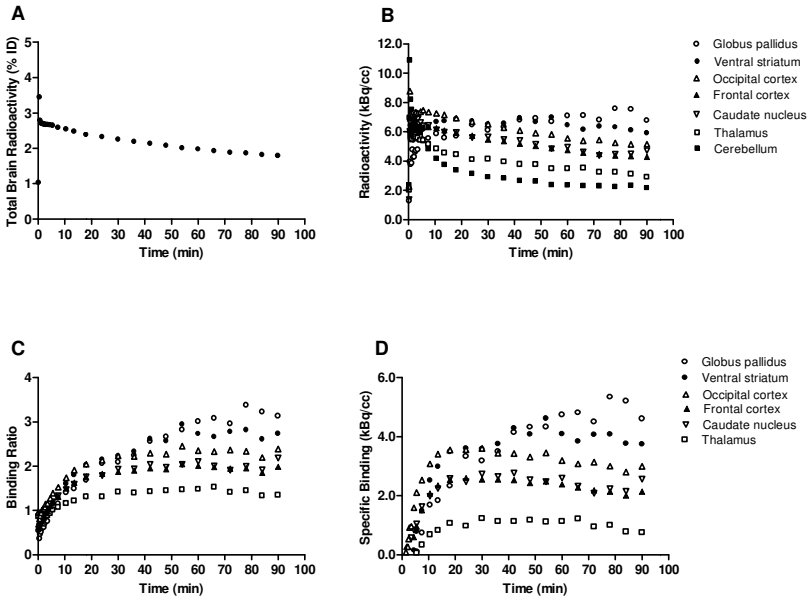

Figure 18. PET-measurement of brain radioactivity after intravenous injection of [^{11}C]AZ10419369 to a healthy volunteer. (A) Total brain radioactivity presented as a percentage of injected dose (ID). (B) Time-activity curves of regional brain radioactivity. (C) Ratios of radioactivity in each of the target region to radioactivity in the cerebellum. (D) Time curves for specific [^{11}C]AZ10419369 binding.

In addition the low rate of radioligand metabolism and no support for formation of active lipophilic metabolites in plasma is an advantage for planned studies aiming at quantitative modeling of [^{11}C]AZ10419369 binding in the human brain.

In parallel with this work, another 5-HT_{1B} PET radioligand, [^{11}C]P943, was developed[112]. [^{11}C]AZ10419369 and [^{11}C]P943 has similar brain uptake (3.5% ID vs 4.2% ID) and similar kinetics in globus pallidus where neither radioligand reaches specific binding equilibrium. One possible difference is that [^{11}C]AZ10419369 reaches specific binding equilibrium earlier in the cortex than what [^{11}C]P943 does (30 min and 80 min respectively).

[^{11}C]AZ10419369 is the first radioligand available for PET determination of 5-HT_{1B} binding *in vivo*. This radioligand may be useful in future studies evaluating drug-induced receptor occupancy, as well as in analyzing possible differences in brain 5-HT_{1B} receptor levels in psychiatric disorders.

5 SUMMARY OF FINDINGS

The studies enclosed in this thesis have shown that in-target produced [^{11}C]CH_4 makes it possible for the routine ^{11}C-labeling of PET radioligands with high SA without any tedious pre-production flushing and cleaning methods necessary. This has especially been demonstrated for radioligands synthesized from [^{11}C]CH_3I but also from [^{11}C]HCN. When in-target produced [^{11}C]CH_4 was used we found an increase in the mean SA of up to 17 times for ^{11}C-methylations and 9 times for ^{11}C-cyanations. In addition, we can assure a sufficiently low mass (high SA) also for high binding affinity (picomolar) radioligands labeled by ^{11}C-methylations, which is low enough to assure less than 5% occupancy.

The proposed mGluR5 radioligand [^{11}C]AR-P135003, was successfully labeled using [^{11}C]HCN both with low SA (from [^{11}C]CO2) and higher SA (from [^{11}C]CH_4). In this first preliminary characterization in cynomolgus monkeys the radioligand was found to enter the brain to a high extent, the binding was saturable and the regional radioactivity pattern was in accordance with the known distribution of mGluR5.

Using high SA [^{11}C]CH_3I we prepared the second generation amyloid radioligand [^{11}C]AZD2184 in a two step radiosynthesis. In non-human primates the radioligand demonstrated a sufficient brain exposure with a relatively lower white matter binding compared to other β-amyloid PET radioligands reported to date.

We also report the development program for a 5-HT_{1B} PET radioligand in which we were able to identify [^{11}C]AZ10419369, the first reported PET radioligand suitable for *in vivo* visualization of 5-HT_{1B} receptors in the primate brain.

In an attempt to draw general conclusions on the relationship between the physicochemical properties of compounds and the effect this imposes in the *in vivo* setting, lipophilicity was found to be an important property showing relation to brain exposure as well as the non-specific binding of the radioligands.

6 FUTURE PERSPECTIVES AND CHALLENGES

1. In this thesis, the in-target production of $[^{11}C]CH_4$ is proposed to be an efficient route for the ^{11}C-labeling of radioligands with high SA. In our laboratory this method is reliable and meets our needs for routine production of ^{11}C-radioligands. However, challenges still remains:

   - The yield from the $[^{11}C]CH_4$ target is relatively low compared to $[^{11}C]CO_2$ targets. In addition the gas phase reaction to produce $[^{11}C]CH_3I$ gives only about 50% conversion using conventional methods. There is a need for a higher total radiochemical yield of $[^{11}C]CH_3I$ from in-target produced $[^{11}C]CH_4$.

   - Not all ^{11}C-radioligands can in a straight-forward way be synthesized from $[^{11}C]CH_4$. ^{11}C-acylations and ^{11}C-carbonylations are examples of two important labeling procedures that are routinely prepared from $[^{11}C]CO_2$. Therefore, there is a need to increase the SA of radioligands produced in routine also from in-target produced $[^{11}C]CO_2$[100, 113, 114].

2. By the discovery of the human genome we know that there are several hundred targets in the CNS that are able to bind small molecules with appropriate properties and would thus be appropriate targets for PET imaging. The development and validation of new radioligands requires a multidisciplinary approach and is of major importance for the expansion of PET. The development of PET radioligands is challenging with respect to many issues. One important topic in PET radioligand development is the predictability concerning which compound will make a good PET radioligand. Further understanding about how the physicochemical and *in vitro* pharmacological properties of compounds relate to the *in vivo* behavior regarding important characteristics such as brain exposure, non-specific binding and metabolism would help the selection of candidate compounds in PET radioligand development programs.

   New radioligands specific for different molecular targets are valuable for basic research, drug development and clinical studies. The collaboration between academia and pharmaceutical industry during the last decade has boosted the development of new molecular PET radioligands and this collaboration is invaluable also for the continuation of successful radioligand development[9, 13]. In addition, new technologies such as microfluidic chemistry might have the ability to speed up the development of new probes.

   Some specific challenges for the PET radioligands developed in this thesis:

   - During the course of this thesis project a new radioligand for PET imaging for mGluR5, $[^{11}C]$ABP688[55], was reported. A human PET study[115] indicated suitable characteristics for imaging of the mGluR5. However, a comparison with the mGluR5 radioligand reported in this thesis, $[^{11}C]$AR-P135003, might give additional and complementary information about the mGluR5. $[^{11}C]$AR-P135003 is especially interesting since it does not depend on the presence of an alkyne moiety

and thus belongs to another unrelated structural class than all other available mGluR5 PET radioligands reported to date.

- [^{11}C]AZD2184 was shown to be a promising radioligand for early detection of β-amyloid depositions in Alzheimer's disease using short scanning protocols. There is a need for a fluorine-18 labeled derivative of [^{11}C]AZD2184, as this would increase the availability of this radioligand to PET centers without an on-site cyclotron.

- We have shown that [^{11}C]AZ10419369 is a useful radioligand for the *in vivo* visualization of 5-HT$_{1B}$ receptors in the human brain. We have recently reported that this radioligand is sensitive to changes in endogenous serotonin concentration[116], which is a research area that needs to be further examined. The evaluation of this radioligand in the research of the pathophysiology of serotonergic diseases is another important topic for future studies.

7 ACKNOWLEDGEMENTS

Many people have contributed in various ways to make this thesis possible. I would like to express my sincere gratitude and appreciation to all of them, and especially I would like to thank:

Professor Christer Halldin, my supervisor, for taking me in as a PhD student, your guidance and interest in this work, as well as unlimited support, encouragement and energy throughout these years.

Professor Lars Farde, my co-supervisor, for guidance, support and valuable comments on manuscripts.

All past and present members of the radiochemistry group at Karolinska Institutet: Phong Truong for excellent technical assistance, being an outstanding office-mate and an even better friend, Sjoerd Finnema, Dr. Magnus Schou and Carsten Steiger for friendship and excellent discussions about science, sports and life, Sangram Nag for being a superb office-mate and teaching me about cricket, Arsalan Amir, Siv Eriksson, Guennadi Jogolev and Kenneth Dahl for excellent technical assistance, Dr. Anu Airaksinen, Dr. Sean Donohue, Dr. Raisa Krasikova, Dr. Zhisheng Jia, Dr. Peter Johnström, Mahabuba Jahan, Dr. Evgeny Shchukin, Jari Tarkiainen, Neil Saigal, Anna Sumic, Linda Bergman, Dr. Ryuji Nakao, Dr. Vladimir Stepanov, Dr. Fabienne Gourand, Dr. Jonas Bergström. Thank you all for your friendship and making the one hour travel from Uppsala easy every day.

All past and present members of the PET imaging group at Karolinska Institutet: Associate professor Bálazs Gulyás, Gudrun Nylén, Dr. Katarina Varnäs, Dr. Nicholas Seneca, Julio Gabriel and Dr. Zsolt Cselényi, for invaluable help with the monkey experiments and image analysis. Associate professor Anna-Lena Nordström, Dr. Per Karlsson, Dr. Jacqueline Borg, Dr. Simon Červenka, Dr. Johan Lundberg, Nils Sjöholm, Dr. Mikael Tiger, Dr. Stefan Pauli, Dr. Hristina Jovanovic, Dr. Judit Sóvágó, Dr. Aurelija Jucaite, Dr. Akihiro Takano, Patrik Mattsson, Dr. Hans Olsson and Dr. Andrea Varrone for creating a friendly atmosphere.

Past and present members of AstraZeneca: Dr. Ed Pierson, Dr. Chad Elmore, Dr. David Wensbo, Dr. Johan Sandell and Dr. Patrick Raboisson for fruitful collaborations.

Karin Zahir, Urban Hansson, Ulla-Kajsa Pehrson, Kjerstin Lind, Johan Molin, Jan Everhov, Pia Schönbeck, Sofia Sjödin, Miklos Toth, Martin Schain, Dr. Mette Skinbjerg and Dr. Garth Terry for being a lovely bunch of people.

Members of the Karolinska Pharmacy PET radiochemistry group: Professor Sharon Stone-Elander, Dr. Jan-Olov Thorell, Dr. Anna Fredriksson, Erik Samen and Emma Jussing for making life fun in the radiochemistry lab.

Martin for getting me out running no matter what and of course for O'Martins, Dr. Do for keeping close contact from Boston, the Friday night poker members, Satyan, Nobby and Rickard and all other friends and my Canadian family: Mike, Penny and Corey for being so warm and kind.

My parents Sven and Marianne for always being there, my brother Per and my sister Lena and their families for your support.

Finally I would like to thank you Candice, for being exactly who you are, for your love and for making me happy.

8 REFERENCES

1. Cassidy, P.J. and G.K. Radda, Molecular imaging perspectives. Journal of The Royal Society Interface, 2005. 2(3): p. 133-144.
2. Ametamey, S.M., M. Honer, and P.A. Schubiger, Molecular imaging with PET. Chem Rev, 2008. 108(5): p. 1501-16.
3. Rahmim, A. and H. Zaidi, PET versus SPECT: strengths, limitations and challenges. Nuclear Medicine Communications, 2008. 29(3): p. 193-207.
4. Meikle, S.R., F.J. Beekman, and S.E. Rose, Complementary molecular imaging technologies: High resolution SPECT, PET and MRI. Drug Discovery Today: Technologies, 2006. 3(2): p. 187-194.
5. Basu, S. and A. Alavi, Unparalleled contribution of 18F-FDG PET to medicine over 3 decades. J Nucl Med, 2008. 49(10): p. 17N-21N, 37N.
6. Guadagno, J.V., E.A. Warburton, P.S. Jones, D.J. Day, F.I. Aigbirhio, T.D. Fryer, S. Harding, C.J. Price, H.A. Green, O. Barret, J.H. Gillard, and J.C. Baron, How affected is oxygen metabolism in DWI lesions?: A combined acute stroke PET-MR study. Neurology, 2006. 67(5): p. 824-9.
7. Morrish, P.K., J.S. Rakshi, D.L. Bailey, G.V. Sawle, and D.J. Brooks, Measuring the rate of progression and estimating the preclinical period of Parkinson's disease with [18F]dopa PET. J Neurol Neurosurg Psychiatry, 1998. 64(3): p. 314-9.
8. Tolboom, N., M. Yaqub, W.M. van der Flier, R. Boellaard, G. Luurtsema, A.D. Windhorst, F. Barkhof, P. Scheltens, A.A. Lammertsma, and B.N. van Berckel, Detection of Alzheimer pathology in vivo using both 11C-PIB and 18F-FDDNP PET. J Nucl Med, 2009. 50(2): p. 191-7.
9. Lee, C.M. and L. Farde, Using positron emission tomography to facilitate CNS drug development. Trends Pharmacol Sci, 2006. 27(6): p. 310-6.
10. CHMP, Committee for medicinal products for human use. Position paper on non-clinical safety studies to support clinical trials with a single microdose. European medicines agency. Evaluation of Medicines for Human Use. , 2004.
11. Gee, A.D., Neuropharmacology and drug development. Br Med Bull, 2003. 65: p. 169-77.
12. Sugiyama, Y., Effective use of microdosing and Positron Emission Tomography (PET) studies on new drug discovery and development. Drug Metab Pharmacokinet, 2009. 24(2): p. 127-9.
13. Halldin, C., B. Gulyas, and L. Farde, PET studies with carbon-11 radioligands in neuropsychopharmacological drug development. Curr Pharm Des, 2001. 7(18): p. 1907-29.
14. Hargreaves, R.J., The role of molecular imaging in drug discovery and development. Clin Pharmacol Ther, 2008. 83(2): p. 349-53.
15. Waterhouse, R.N., Determination of lipophilicity and its use as a predictor of blood-brain barrier penetration of molecular imaging agents. Mol Imaging Biol, 2003. 5(6): p. 376-89.
16. Laruelle, M., M. Slifstein, and Y. Huang, Relationships between radiotracer properties and image quality in molecular imaging of the brain with positron emission tomography. Mol Imaging Biol, 2003. 5(6): p. 363-75.
17. Pike, V.W., PET radiotracers: crossing the blood-brain barrier and surviving metabolism. Trends in Pharmacological Sciences, 2009. 30(8): p. 431-440.

18. Halldin, C., B. Gulyas, O. Langer, and L. Farde, Brain radioligands--state of the art and new trends. Q J Nucl Med, 2001. 45(2): p. 139-52.
19. Elsinga, P.H., Radiopharmaceutical chemistry for positron emission tomography. Methods, 2002. 27(3): p. 208-17.
20. Buckley, K., J. Huser, S. Jivan, K. Chun, and T. Ruth, 11C-methane production in small volume, high pressure gas targets. Radiochim, Acta, 2000. 88: p. 201-205.
21. Litkenhous, E., E. and C. Mann, A., Hydrogenation of Nickel Carbonyl. Ind. Eng. Chem., 1937. 29(8): p. 934-938.
22. Landais, P. and R. Finn, On-line preparation of [11C]carbon dioxide from [11C]methane. Int J Rad Appl Instrum A, 1989. 40(3): p. 265-6.
23. Langstrom, B. and H. Lundqvist, The preparation of 11C-methyl iodide and its use in the synthesis of 11C-methyl-L-methionine. Int J Appl Radiat Isot, 1976. 27(7): p. 357-63.
24. Link, J.M., K.A. Krohn, and J.C. Clark, Production of [11C]CH3I by single pass reaction of [11C]CH4 with I2. Nucl Med Biol, 1997. 24(1): p. 93-7.
25. Noguchi, J. and K. Suzuki, Automated synthesis of the ultra high specific activity of [11C]Ro15-4513 and its application in an extremely low concentration region to an ARG study. Nucl Med Biol, 2003. 30(3): p. 335-43.
26. Larsen, P., J. Ulin, K. Dahlstrom, and M. Jensen, Synthesis of C-11 iodomethane by iodination of C-11 methane. Applied Radiation and Isotopes, 1997. 48(2): p. 153-157.
27. Iwata, R., T. Ido, T. Takahashi, H. Nakanishi, and S. Iida, Optimization of [11C]HCN production and no-carrier-added [1-11C]amino acid synthesis. Int J Rad Appl Instrum A, 1987. 38(2): p. 97-102.
28. Jewett, D.M., A Simple Synthesis of [C-11] Methyl Triflate. Applied Radiation and Isotopes, 1992. 43(11): p. 1383-1385.
29. Nagren, K., C. Halldin, C.G. Swahn, K.O. Schoeps, O. Langer, M. Mitterhauser, and I. Zolle, Some new methods for the synthesis of cardiac neurotransmission PET radiotracers. Nucl Med Biol, 1995. 22(8): p. 1037-43.
30. Kihlberg, T., P. Gullberg, and B. Langstrom, [C-11] Methylenetriphenylphosphorane, a New C-11 Precursor, Used in a One-Pot Wittig Synthesis of [Beta-C-11]Styrene. Journal of Labelled Compounds & Radiopharmaceuticals, 1990. 28(10): p. 1115-1120.
31. Hostetler, E.D., G.E. Terry, and H.D. Burns, An improved synthesis of substituted [C-11]toluenes via Suzuki coupling with [C-11] methyl iodide. Journal of Labelled Compounds & Radiopharmaceuticals, 2005. 48(9): p. 629-634.
32. Bourdier, T., M. Huiban, F. Sobrio, C. Perrio, and L. Barre, Tetra- or Mono-Organotin Reagents in the Stille Reaction for the Labelling of Potential Radiotracers with Carbon-11: A Comparative Study. Journal of Labelled Compounds & Radiopharmaceuticals, 2005. 48: p. S173-S173.
33. Reiffers, S., W. Vaalburg, T. Wiegman, H.D. Beerlingvandermolen, A.M.J. Paans, M.G. Woldring, and H. Wynberg, Methyllithium-C-11 - New Synthetic Tool in Radiopharmaceutical Chemistry. Journal of Labelled Compounds & Radiopharmaceuticals, 1979. 16(1): p. 56-58.
34. Schoeps, K.O., S. Stoneelander, and C. Halldin, Online Synthesis of [C-11] Nitroalkanes. Applied Radiation and Isotopes, 1989. 40(3): p. 261-262.
35. McCarron, J.A. and V.W. Pike, Synthesis of no-carrier-added [C-11]methanesulfonyl chloride as a new labeling agent for PET

radiopharmaceutical development. Journal of Labelled Compounds & Radiopharmaceuticals, 2003. 46(12): p. 1127-1140.
36. Elsinga, P.H., E. Keller, T.J. Degroot, G.M. Visser, and W. Vaalburg, Synthesis of [C-11] Methyl Magnesium Iodide and Its Application to the Introduction of [C-11] N-Tert-Butyl Groups and [C-11]-Sec-Alcohols. Applied Radiation and Isotopes, 1995. 46(4): p. 227-231.
37. Zessin, J., J. Steinbach, and B. Johannsen, Synthesis of triphenylarsonium [C-11]methylide, a new C-11-precursor. Application in the preparation of [2-C-11]indole. Journal of Labelled Compounds & Radiopharmaceuticals, 1999. 42(8): p. 725-736.
38. Antoni, G., T. Kihlberg, and B. Långström, Aspects on the Synthesis of 11C-Labelled Compounds, in Handbook of Radiopharmaceuticals, C.S.R. Michael J. Welch, Editor. 2004. p. 141-194.
39. Olsson, H., C. Halldin, and L. Farde, Differentiation of extrastriatal dopamine D2 receptor density and affinity in the human brain using PET. Neuroimage, 2004. 22(2): p. 794-803.
40. Bergman, J., O. Eskola, P. Lehikoinen, and O. Solin, Automated synthesis and purification of [18F]bromofluoromethane at high specific radioactivity. Appl Radiat Isot, 2001. 54(6): p. 927-33.
41. Christman, D., Finn, RD., Karlstrom, KI., Wolf, AP., The production of ultra high activity 11C-labeled hydrogen cyanide, carbon dioxide, carbon monoxide and methane via the 14N(p,a)11C reaction (XV). International Journal of Applied Radiation and Isotopes, 1975. 26: p. 435-442.
42. Iwata, R., T. Ido, A. Ujiie, T. Takahashi, K. Ishiwata, K. Hatano, and M. Sugahara, Comparative study of specific activity of [11C]CH3I: Search for a source of carrier carbons. Appl. Radiat. Isot., 1988. 39: p. 1-7.
43. Spooren, W.P., F. Gasparini, T.E. Salt, and R. Kuhn, Novel allosteric antagonists shed light on mglu(5) receptors and CNS disorders. Trends Pharmacol Sci, 2001. 22(7): p. 331-7.
44. Bradbury, M.J., D.R. Giracello, D.F. Chapman, G. Holtz, H. Schaffhauser, S.P. Rao, M.A. Varney, and J.J. Anderson, Metabotropic glutamate receptor 5 antagonist-induced stimulation of hypothalamic-pituitary-adrenal axis activity: interaction with serotonergic systems. Neuropharmacology, 2003. 44(5): p. 562-72.
45. Ohnuma, T., S.J. Augood, H. Arai, P.J. McKenna, and P.C. Emson, Expression of the human excitatory amino acid transporter 2 and metabotropic glutamate receptors 3 and 5 in the prefrontal cortex from normal individuals and patients with schizophrenia. Brain Res Mol Brain Res, 1998. 56(1-2): p. 207-17.
46. Rouse, S.T., M.J. Marino, S.R. Bradley, H. Awad, M. Wittmann, and P.J. Conn, Distribution and roles of metabotropic glutamate receptors in the basal ganglia motor circuit: implications for treatment of Parkinson's disease and related disorders. Pharmacol Ther, 2000. 88(3): p. 427-35.
47. Westmark, C.J., P.R. Westmark, and J.S. Malter, MPEP reduces seizure severity in Fmr-1 KO mice over expressing human Abeta. Int J Clin Exp Pathol, 2009. 3(1): p. 56-68.
48. Chiamulera, C., M.P. Epping-Jordan, A. Zocchi, C. Marcon, C. Cottiny, S. Tacconi, M. Corsi, F. Orzi, and F. Conquet, Reinforcing and locomotor stimulant effects of cocaine are absent in mGluR5 null mutant mice. Nat Neurosci, 2001. 4(9): p. 873-4.
49. Notenboom, R.G., D.R. Hampson, G.H. Jansen, P.C. van Rijen, C.W. van Veelen, O. van Nieuwenhuizen, and P.N. de Graan, Up-regulation of

hippocampal metabotropic glutamate receptor 5 in temporal lobe epilepsy patients. Brain, 2006. 129(Pt 1): p. 96-107.
50. Pin, J.P. and R. Duvoisin, The metabotropic glutamate receptors: structure and functions. Neuropharmacology, 1995. 34(1): p. 1-26.
51. Gasparini, F., K. Lingenhohl, N. Stoehr, P.J. Flor, M. Heinrich, I. Vranesic, M. Biollaz, H. Allgeier, R. Heckendorn, S. Urwyler, M.A. Varney, E.C. Johnson, S.D. Hess, S.P. Rao, A.I. Sacaan, E.M. Santori, G. Velicelebi, and R. Kuhn, 2-Methyl-6-(phenylethynyl)-pyridine (MPEP), a potent, selective and systemically active mGlu5 receptor antagonist. Neuropharmacology, 1999. 38(10): p. 1493-503.
52. Cosford, N.D., L. Tehrani, J. Roppe, E. Schweiger, N.D. Smith, J. Anderson, L. Bristow, J. Brodkin, X. Jiang, I. McDonald, S. Rao, M. Washburn, and M.A. Varney, 3-[(2-Methyl-1,3-thiazol-4-yl)ethynyl]-pyridine: a potent and highly selective metabotropic glutamate subtype 5 receptor antagonist with anxiolytic activity. J Med Chem, 2003. 46(2): p. 204-6.
53. Pagano, A., D. Ruegg, S. Litschig, N. Stoehr, C. Stierlin, M. Heinrich, P. Floersheim, L. Prezeau, F. Carroll, J.P. Pin, A. Cambria, I. Vranesic, P.J. Flor, F. Gasparini, and R. Kuhn, The non-competitive antagonists 2-methyl-6-(phenylethynyl)pyridine and 7-hydroxyiminocyclopropan[b]chromen-1a-carboxylic acid ethyl ester interact with overlapping binding pockets in the transmembrane region of group I metabotropic glutamate receptors. J Biol Chem, 2000. 275(43): p. 33750-8.
54. Romano, C., M.A. Sesma, C.T. McDonald, K. O'Malley, A.N. Van den Pol, and J.W. Olney, Distribution of metabotropic glutamate receptor mGluR5 immunoreactivity in rat brain. J Comp Neurol, 1995. 355(3): p. 455-69.
55. Ametamey, S.M., L.J. Kessler, M. Honer, M.T. Wyss, A. Buck, S. Hintermann, Y.P. Auberson, F. Gasparini, and P.A. Schubiger, Radiosynthesis and preclinical evaluation of 11C-ABP688 as a probe for imaging the metabotropic glutamate receptor subtype 5. J Nucl Med, 2006. 47(4): p. 698-705.
56. Hamill, T.G., S. Krause, C. Ryan, C. Bonnefous, S. Govek, T.J. Seiders, N.D. Cosford, J. Roppe, T. Kamenecka, S. Patel, R.E. Gibson, S. Sanabria, K. Riffel, W. Eng, C. King, X. Yang, M.D. Green, S.S. O'Malley, R. Hargreaves, and H.D. Burns, Synthesis, characterization, and first successful monkey imaging studies of metabotropic glutamate receptor subtype 5 (mGluR5) PET radiotracers. Synapse, 2005. 56(4): p. 205-16.
57. Hampel, H., K. Burger, S.J. Teipel, A.L. Bokde, H. Zetterberg, and K. Blennow, Core candidate neurochemical and imaging biomarkers of Alzheimer's disease. Alzheimers Dement, 2008. 4(1): p. 38-48.
58. Selkoe, D.J., Alzheimer's disease: genes, proteins, and therapy. Physiol Rev, 2001. 81(2): p. 741-66.
59. Klunk, W.E., H. Engler, A. Nordberg, Y. Wang, G. Blomqvist, D.P. Holt, M. Bergstrom, I. Savitcheva, G.F. Huang, S. Estrada, B. Ausen, M.L. Debnath, J. Barletta, J.C. Price, J. Sandell, B.J. Lopresti, A. Wall, P. Koivisto, G. Antoni, C.A. Mathis, and B. Langstrom, Imaging brain amyloid in Alzheimer's disease with Pittsburgh Compound-B. Ann Neurol, 2004. 55(3): p. 306-19.
60. Pike, K.E., G. Savage, V.L. Villemagne, S. Ng, S.A. Moss, P. Maruff, C.A. Mathis, W.E. Klunk, C.L. Masters, and C.C. Rowe, Beta-amyloid imaging and memory in non-demented individuals: evidence for preclinical Alzheimer's disease. Brain, 2007. 130(Pt 11): p. 2837-44.
61. Forsberg, A., H. Engler, O. Almkvist, G. Blomquist, G. Hagman, A. Wall, A. Ringheim, B. Langstrom, and A. Nordberg, PET imaging of amyloid deposition

in patients with mild cognitive impairment. Neurobiol Aging, 2008. 29(10): p. 1456-65.
62. Johnson, A.E., Jeppsson, F., Sandell, J., Wensbo, D., Neelissen, J. A. M., Juréus, A., Ström, P., Norman, H., Farde, L., Svensson, S. P. S., AZD2184 - a radioligand for sensitive detection of β-amyloid deposits. Journal of Neurochemistry, 2009. 108: p. 1177-1186.
63. Hoyer, D., J.P. Hannon, and G.R. Martin, Molecular, pharmacological and functional diversity of 5-HT receptors. Pharmacol Biochem Behav, 2002. 71(4): p. 533-54.
64. Engel, G., M. Gothert, D. Hoyer, E. Schlicker, and K. Hillenbrand, Identity of inhibitory presynaptic 5-hydroxytryptamine (5-HT) autoreceptors in the rat brain cortex with 5-HT1B binding sites. Naunyn Schmiedebergs Arch Pharmacol, 1986. 332(1): p. 1-7.
65. Sarhan, H., B. Grimaldi, R. Hen, and G. Fillion, 5-HT1B receptors modulate release of [3H]dopamine from rat striatal synaptosomes: further evidence using 5-HT moduline, polyclonal 5-HT1B receptor antibodies and 5-HT1B receptor knock-out mice. Naunyn Schmiedebergs Arch Pharmacol, 2000. 361(1): p. 12-8.
66. Maura, G., E. Roccatagliata, and M. Raiteri, Serotonin autoreceptor in rat hippocampus: pharmacological characterization as a subtype of the 5-HT1 receptor. Naunyn Schmiedebergs Arch Pharmacol, 1986. 334(4): p. 323-6.
67. Barnes, N.M. and T. Sharp, A review of central 5-HT receptors and their function. Neuropharmacology, 1999. 38(8): p. 1083-152.
68. Sari, Y., Serotonin1B receptors: from protein to physiological function and behavior. Neurosci Biobehav Rev, 2004. 28(6): p. 565-82.
69. Gingrich, J.A. and R. Hen, Dissecting the role of the serotonin system in neuropsychiatric disorders using knockout mice. Psychopharmacology (Berl), 2001. 155(1): p. 1-10.
70. Garcia-Alloza, M., W.D. Hirst, C.P. Chen, B. Lasheras, P.T. Francis, and M.J. Ramirez, Differential involvement of 5-HT(1B/1D) and 5-HT6 receptors in cognitive and non-cognitive symptoms in Alzheimer's disease. Neuropsychopharmacology, 2004. 29(2): p. 410-6.
71. Stenfors, C., C. Ahlgren, H. Yu, M. Weden, L.G. Larsson, and S.B. Ross, Effects of long-term administration of the 5-hydroxytryptamine1B receptor antagonist AR-A000002 to guinea pigs. Psychopharmacology (Berl), 2004. 172(3): p. 333-40.
72. Hudzik, T.J., M. Yanek, T. Porrey, J. Evenden, C. Paronis, M. Mastrangelo, C. Ryan, S. Ross, and C. Stenfors, Behavioral pharmacology of AR-A000002, a novel, selective 5-hydroxytryptamine(1B) antagonist. J Pharmacol Exp Ther, 2003. 304(3): p. 1072-84.
73. Bonaventure, P., A. Schotte, P. Cras, and J.E. Leysen, Autoradiographic mapping of 5-HT1B- and 5-HT1D receptors in human brain using [3H]alniditan, a new radioligand. Receptors Channels, 1997. 5(3-4): p. 225-30.
74. Varnas, K., H. Hall, P. Bonaventure, and G. Sedvall, Autoradiographic mapping of 5-HT(1B) and 5-HT(1D) receptors in the post mortem human brain using [(3)H]GR 125743. Brain Res, 2001. 915(1): p. 47-57.
75. Schlicker, E., K. Fink, G.J. Molderings, G.W. Price, M. Duckworth, L. Gaster, D.N. Middlemiss, J. Zentner, J. Likungu, and M. Gothert, Effects of selective h5-HT1B (SB-216641) and h5-HT1D (BRL-15572) receptor ligands on guinea-

pig and human 5-HT auto- and heteroreceptors. Naunyn Schmiedebergs Arch Pharmacol, 1997. 356(3): p. 321-7.
76. Bruinvels, A.T., B. Landwehrmeyer, E.L. Gustafson, M.M. Durkin, G. Mengod, T.A. Branchek, D. Hoyer, and J.M. Palacios, Localization of 5-HT1B, 5-HT1D alpha, 5-HT1E and 5-HT1F receptor messenger RNA in rodent and primate brain. Neuropharmacology, 1994. 33(3-4): p. 367-86.
77. Peterlin, B.L. and A.M. Rapoport, Clinical pharmacology of the serotonin receptor agonist, zolmitriptan. Expert Opin Drug Metab Toxicol, 2007. 3(6): p. 899-911.
78. Clitherow, J.W., D.I. Scopes, M. Skingle, C.C. Jordan, W. Feniuk, I.B. Campbell, M.C. Carter, E.W. Collington, H.E. Connor, G.A. Higgins, and et al., Evolution of a novel series of [(N,N-dimethylamino)propyl]- and piperazinylbenzanilides as the first selective 5-HT1D antagonists. J Med Chem, 1994. 37(15): p. 2253-7.
79. Gaster, L.M., F.E. Blaney, S. Davies, D.M. Duckworth, P. Ham, S. Jenkins, A.J. Jennings, G.F. Joiner, F.D. King, K.R. Mulholland, P.A. Wyman, J.J. Hagan, J. Hatcher, B.J. Jones, D.N. Middlemiss, G.W. Price, G. Riley, C. Roberts, C. Routledge, J. Selkirk, and P.D. Slade, The selective 5-HT1B receptor inverse agonist 1'-methyl-5-[[2'-methyl-4'-(5-methyl-1,2, 4-oxadiazol-3-yl)biphenyl-4-yl]carbonyl]-2,3,6,7-tetrahydro- spiro[furo[2,3-f]indole-3,4'-piperidine] (SB-224289) potently blocks terminal 5-HT autoreceptor function both in vitro and in vivo. J Med Chem, 1998. 41(8): p. 1218-35.
80. Audinot, V., S. Lochon, A. Newman-Tancredi, G. Lavielle, and M.J. Millan, Binding profile of the novel 5-HT1B/1D receptor antagonist, [3H]GR 125,743, in guinea-pig brain: a comparison with [3H]5-carboxamidotryptamine. Eur J Pharmacol, 1997. 327(2-3): p. 247-56.
81. Ahlgren, C., A. Eriksson, P. Tellefors, S.B. Ross, C. Stenfors, and A. Malmberg, In vitro characterization of AR-A000002, a novel 5-hydroxytryptamine(1B) autoreceptor antagonist. Eur J Pharmacol, 2004. 499(1-2): p. 67-75.
82. Sandell, J., O. Langer, P. Larsen, F. Dolle, F. Vaufrey, S. Demphel, C. Crouzel, and C. Halldin, Improved specific radioactivity of the PET radioligand [11C]FLB 457 by use of the GE medical systems PETtrace MeI MicroLab. J Labelled Compd Radiopharm, 2000. 43: p. 331-338.
83. Clark, J.D., G.F. Gebhart, J.C. Gonder, M.E. Keeling, and D.F. Kohn, Special Report: The 1996 Guide for the Care and Use of Laboratory Animals. ILAR J, 1997. 38(1): p. 41-48.
84. Karlsson, P., L. Farde, C. Halldin, C.G. Swahn, G. Sedvall, C. Foged, K.T. Hansen, and B. Skrumsager, PET examination of [^{11}C]NNC 687 and [^{11}C]NNC 756 as new radioligands for the D_1-dopamine receptor. Psychopharmacology (Berl), 1993. 113: p. 149-156.
85. Wienhard, K., M. Dahlbom, L. Eriksson, C. Michel, T. Bruckbauer, U. Pietrzyk, and W.D. Heiss, The ECAT EXACT HR: performance of a new high resolution positron scanner. J Comput Assist Tomogr, 1994. 18(1): p. 110-8.
86. Ito, H., J. Hietala, G. Blomqvist, C. Halldin, and L. Farde, Comparison of the transient equilibrium and continuous infusion method for quantitative PET analysis of [11C]raclopride binding. J Cereb Blood Flow Metab, 1998. 18(9): p. 941-50.
87. Halldin, C., C. Swahn, L. Farde, and G. Sedvall, Radioligand disposition and metabolism -Key information in early drug development, in PET for drug

development and evaluation, D. Comar, Editor. 1995, Klüwer Academic Publishers: Dordrecht. p. 55-65.
88. Langer, O., K. Nagren, F. Dolle, C. Lundkvist, J. Sandell, C.G. Swahn, F. Vaufrey, C. Crouzel, B. Maziere, and C. Halldin, Precursor synthesis and radiolabelling of the dopamine D-2 receptor ligand C-11 raclopride from C-11 methyl triflate. J Label Compd Radiopharm, 1999. 42(12): p. 1183-1193.
89. Ehrin, E., L. Farde, T. Depaulis, L. Eriksson, T. Greitz, P. Johnstrom, J.E. Litton, J.L.G. Nilsson, G. Sedvall, S. Stoneelander, and S.O. Ogren, Preparation of C-11-Labelled Raclopride, a New Potent Dopamine Receptor Antagonist - Preliminary Pet Studies of Cerebral Dopamine-Receptors in the Monkey. International Journal of Applied Radiation and Isotopes, 1985. 36(4): p. 269-&.
90. Halldin, C., J. Lundberg, J. Sovago, B. Gulyas, D. Guilloteau, J. Vercouillie, P. Emond, S. Chalon, J. Tarkiainen, J. Hiltunen, and L. Farde, [(11)C]MADAM, a new serotonin transporter radioligand characterized in the monkey brain by PET. Synapse, 2005. 58(3): p. 173-83.
91. Halldin, C., N. Erixon-Lindroth, S. Pauli, Y.H. Chou, Y. Okubo, P. Karlsson, C. Lundkvist, H. Olsson, D. Guilloteau, P. Emond, and L. Farde, [(11)C]PE2I: a highly selective radioligand for PET examination of the dopamine transporter in monkey and human brain. Eur J Nucl Med Mol Imaging, 2003. 30(9): p. 1220-30.
92. Halldin, C., L. Farde, T. Hogberg, N. Mohell, H. Hall, T. Suhara, P. Karlsson, Y. Nakashima, and C.G. Swahn, Carbon-11-FLB 457: a radioligand for extrastriatal D2 dopamine receptors. J Nucl Med, 1995. 36(7): p. 1275-81.
93. Sandell, J., O. Langer, P. Larsen, F. Dolle, F. Vaufrey, S. Demphel, C. Crouzel, and C. Halldin, Improved specific radioactivity of the PET radioligand [11C]FLB 457 by use of the GE medical systems PETtrace MeI MicroLab. J Label Compd Radiopharm, 2000. 43: p. 331-338.
94. Nagren, K., L. Muller, C. Halldin, C.G. Swahn, and P. Lehikoinen, Improved Synthesis of Some Commonly Used Pet Radioligands by the Use of [C-11] Methyl Triflate. Nuclear Medicine and Biology, 1995. 22(2): p. 235-239.
95. Jacobson, O. and E. Mishani, [11C]-dimethylamine as a labeling agent for PET biomarkers. Appl Radiat Isot, 2008. 66(2): p. 188-93.
96. Gao, M., M. Wang, and Q.H. Zheng, Synthesis of carbon-11 labeled 1-(3,4-dimethoxybenzyl)-2,2-dimethyl-1,2,3,4-tetrahydroisoquinolinium derivatives as new potential PET SKCa channel imaging agents. Appl Radiat Isot, 2008. 66(2): p. 194-202.
97. Kniess, T., K. Rode, and F. Wuest, Practical experiences with the synthesis of [(11)C]CH(3)I through gas phase iodination reaction using a TRACERlabFX(C) synthesis module. Appl Radiat Isot, 2008. 66(4): p. 482-8.
98. Gao, M., M. Wang, B.H. Mock, K.D. Miller, G.W. Sledge, G.D. Hutchins, and Q.H. Zheng, Synthesis of new carbon-11 labeled cyclofenil derivatives for PET imaging of breast cancer estrogen receptors. Appl Radiat Isot, 2008. 66(4): p. 523-9.
99. Wang, M., J.Q. Wang, M. Gao, and Q.H. Zheng, Facile synthesis of new carbon-11 labeled conformationally restricted rivastigmine analogues as potential PET agents for imaging AChE and BChE enzymes. Appl Radiat Isot, 2008. 66(4): p. 506-12.
100. Ermert, J., S. Stusgen, M. Lang, W. Roden, and H.H. Coenen, High molar activity of [(11)C]TCH346 via [(11)C]methyl triflate using the "wet" [(11)C]CO(2) reduction method. Appl Radiat Isot, 2008. 66(5): p. 619-24.

101. Ponchant, M., F. Hinnen, S. Demphel, and C. Crouzel, [C-11]Copper(I) cyanide: A new radioactive precursor for C-11-cyanation and functionalization of haloarenes. Applied Radiation and Isotopes, 1997. 48(6): p. 755-762.
102. Andersson, Y. and B. Långström, Transition metal-mediated reactions using [11C]cyanide in synthesis of 11C-labelled aromatic compounds. J. Chem. Soc., Perkin Trans. 1, 1994: p. 1395-1400.
103. Simeon, F., F. Sobrio, F. Gourand, and L. Barre, Total synthesis and radiolabelling of an efficient rt-PA inhibitor: [C-11] (Z,Z)-BABCH. A first route to [C-11] labelled amidines. Journal of the Chemical Society-Perkin Transactions 1, 2001(7): p. 690-694.
104. Kunzel, S., A. Schweinitz, S. Reissmann, J. Sturzebecher, and T. Steinmetzer, 4-amidinobenzylamine-based inhibitors of urokinase. Bioorg Med Chem Lett, 2002. 12(4): p. 645-8.
105. Ho, J.Z., T.S. Gibson, and J.E. Semple, Novel, Potent Non-Covalent Thrombin Inhibitors Incorporating P3-Lactam Scaffolds. Bioorganic & Medicinal Chemistry Letters, 2002. 12(5): p. 743-748.
106. Corey, E.J. and Venkates.A, Protection of Hydroxyl Groups as Tert-Butyldimethylsilyl Derivatives. Journal of the American Chemical Society, 1972. 94(17): p. 6190-&.
107. Mathis, C.A., Y. Wang, D.P. Holt, G.F. Huang, M.L. Debnath, and W.E. Klunk, Synthesis and evaluation of 11C-labeled 6-substituted 2-arylbenzothiazoles as amyloid imaging agents. J Med Chem, 2003. 46(13): p. 2740-54.
108. ICRP, ICRP publication 73, Radiological protection and safety in medicine. . 1996: Oxford: Permagon Press.
109. Scheinin, N.M., T.K. Tolvanen, I.A. Wilson, E.M. Arponen, K.A. Nagren, and J.O. Rinne, Biodistribution and radiation dosimetry of the amyloid imaging agent 11C-PIB in humans. J Nucl Med, 2007. 48(1): p. 128-33.
110. European-Comission, Radiation protection 99 - Guidance on Medical Exposures in Medical and Biomedical Research. 1998: European Commission.
111. Maier, D.L., C. Sobotka-Briner, M. Ding, M.E. Powell, Q. Jiang, G. Hill, J.R. Heys, C.S. Elmore, M.E. Pierson, and L. Mrzljak, [N-methyl-3H3]AZ10419369 binding to the 5-HT1B receptor: in vitro characterization and in vivo receptor occupancy. J Pharmacol Exp Ther, 2009. 330(1): p. 342-51.
112. Gallezot, J.D., N. Nabulsi, A. Neumeister, B. Planeta-Wilson, W.A. Williams, T. Singhal, S. Kim, R.P. Maguire, T. McCarthy, J.J. Frost, Y. Huang, Y.S. Ding, and R.E. Carson, Kinetic modeling of the serotonin 5-HT(1B) receptor radioligand [(11)C]P943 in humans. J Cereb Blood Flow Metab. 30(1): p. 196-210.
113. Suzuki, K., T. Yamazaki, M. Sasaki, and A. Kubodera, Specific activity of [C-11]CO2 generated in a N-2 gas target: effect of irradiation dose, irradiation history, oxygen content and beam energy. Radiochimica Acta, 2000. 88(3-4): p. 211-215.
114. Eriksson, J., R. Mooij, F.L. Buijs, B. Lambert, L.F. Van Rooij, P.S. Kruijer, and A.D. Windhorst, In Pursuit of [11C]Carbon Dioxide with Increased Specific Activity. Journal of Labelled Compounds & Radiopharmaceuticals, 2009. 52: p. S60-S60.
115. Ametamey, S.M., V. Treyer, J. Streffer, M.T. Wyss, M. Schmidt, M. Blagoev, S. Hintermann, Y. Auberson, F. Gasparini, U.C. Fischer, and A. Buck, Human PET studies of metabotropic glutamate receptor subtype 5 with 11C-ABP688. J Nucl Med, 2007. 48(2): p. 247-52.

116. Finnema, S.J., A. Varrone, T.J. Hwang, B. Gulyás, M.E. Pierson, C. Halldin, and L. Farde, Fenfluramine induced serotonin release decreases [11C]AZ10419369 binding to 5-HT1B-receptors in the primate brain. Synapse, 2010. In Press.